A Passive Current Sharing Method With Common Inductor Multiphase *LLC* Resonant Converter

Hongliang Wang, *Senior Member, IEEE*, Yang Chen, *Student Member, IEEE*, Yan-Fei Liu, *Fellow, IEEE*, Jahangir Afsharian, and Zhihua Yang

***Abstract*—In this paper, a new common inductor current sharing method is proposed for a multiphase *LLC* resonant converter for high-power applications. Automatic current sharing is achieved by using a common resonant inductor connecting the resonant inductors in each *LLC* phase in parallel. The current sharing performance of the proposed method is evaluated under first harmonic approximation (FHA) assumption. The proposed method can automatically share the primary resonant current and the load current for all phases without any additional circuit and control strategy. A 600-W two-phase *LLC* converter prototype based on the proposed method is built to verify the feasibility. Excellent current sharing performance (less than 0.5% current sharing error at full load) has been achieved.**

***Index Terms*—Current sharing error, multiphase *LLC*, resonant converter.**

I. Introduction

RESONANT converter is attractive for isolated dc/dc applications, such as flat-panel TVs, laptop adapters, servers, etc., because of its attractive features: smooth waveforms, high efficiency, and high power density. *LLC* resonant converter has been widely used due to the high efficiency as a result of the zero-voltage switching for the primary-side MOSFET and zero-current switching for the secondary-side diodes [1]–[6]. Other resonant converters, such as *LCC* [7]–[10], *LCLC* [11]–[15], are also used for industry applications. For resonant converter used in high-power applications, high current stress on the power devices may reduce both efficiency and reliability. Multiphase parallel technique can solve this problem by reducing the current stress in each phase [16]–[19]. However, due to the tolerance of resonant components, the resonant frequency of each individual *LLC* phase will be different, thus the output currents will be uneven [20]–[22]. It is observed that a small component tolerance (e.g., 5%) can cause significant current imbalance among phases, such as more than 50% current sharing error and, thus, degradation of the benefits achieved by parallel technique. Therefore, current sharing strategy is mandatory in multiphase *LLC* converter.

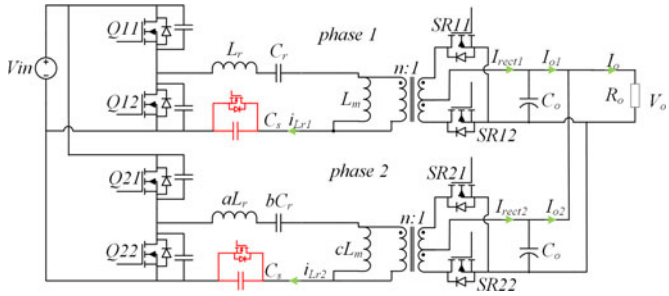

Fig. 1. Switch-controlled capacitor multiphase *LLC* converter.

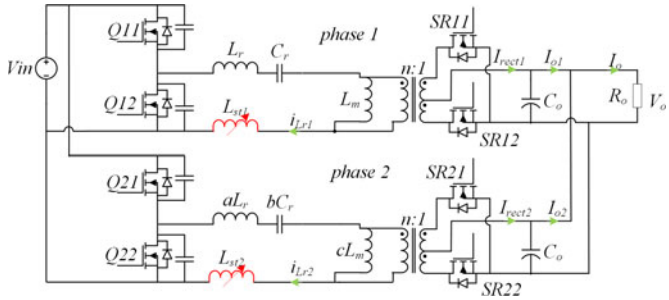

Fig. 2. Linearly controlled inductor multiphase *LLC* converter.

Three types of methods have been used to achieve current sharing for multiphase *LLC* converters [23]–[31]. The first method is the active method, which adjusts the equivalent resonant capacitor [23]–[25] or resonant inductor [26] to compensate the components' tolerances using additional MOSFETs. The circuit diagram with switch-controlled capacitor is shown in Fig. 1. The circuit diagram with linearly controlled inductor is shown in Fig. 2, where the value of the resonant inductor is controlled by an additional dc winding. Parameters *a, b,* and *c* are used to indicate the tolerances between every two phases. Good load sharing performance can be achieved. However, these methods suffer from high cost, complex control, and nonexcellent dynamic performance caused by the sensing circuit and control loop.

The second method is dc voltage self-balanced method based on series input capacitors [27], [28], [32], which is shown in Fig. 3. Ideally, for two-phase, the two input dc capacitor voltages are the same, and equal to half of the input bus voltage. If the load power is not shared, the midpoint voltage will be changed according to each phase's power. With this method, the system has low cost and good load current sharing performance.

Manuscript received May 12, 2016; revised August 23, 2016; accepted October 21, 2016. Date of publication November 8, 2016; date of current version April 24, 2017. This paper was presented in part at the *IEEE Energy Conversion Congress and Exposition*, September 2015, titled as "A common inductor multi-phase LLC resonant converter." Recommended for publication by Associate Editor R.-L. Lin. *(Corresponding author: Yan-Fei Liu.)*

H. Wang, Y. Chen, and Y.-F. Liu are with the Department of Electrical and Computer Engineering, Queen's University, Kingston, ON K7L 3Y4, Canada (e-mail: hongliang.wang@queensu.ca; yang.chen@queensu.ca; yanfei.liu@queensu.ca).

J. Afsharian and Z. Yang are with Murata Power Solutions, Toronto, ON L3R 0J3, Canada (e-mail: jafsharian@murata.com; ZYang@murata.com).

Color versions of one or more of the figures in this paper are available online at http://ieeexplore.ieee.org.

Digital Object Identifier 10.1109/TPEL.2016.2626312

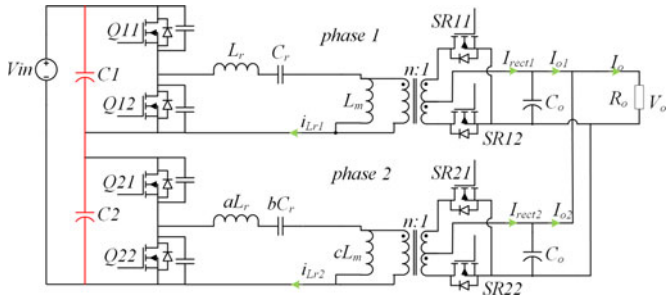

Fig. 3. Series dc capacitor multiphase *LLC* converter.

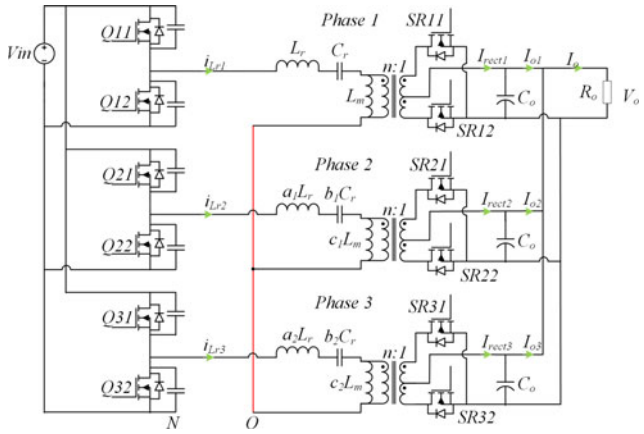

Fig. 4. Three-wire three-phase *LLC* converter.

However, it is not suitable for modularization design in system level, as the input voltage for each phase is reduced with module number increasing. Furthermore, the gate drive circuit for the top phase is complicated. In addition, the relative analysis [32] shows that 29% current sharing error can be achieved under +10% tolerance of resonant inductor, which is not very good.

The third method is using the three-phase three-wire structure for a three-phase *LLC* resonant converter based on 120° phase shift, as shown in Fig. 4, which has good load current sharing near resonant frequency [30], [31], but it is only suitable for converters with three *LLC* modules in parallel. The load current will not share very well when the number of parallel modules is more than three.

Therefore, from the above review, it is noted that the existing technologies cannot provide cost-effective, flexible current sharing performance for multiphase *LLC* resonant converters.

In this paper, a common inductor multiphase *LLC* resonant converter is proposed. The resonant inductor in each *LLC* phase is connected in parallel to achieve current sharing. First harmonic analysis (FHA) shows that the load current of each phase can be automatically shared. This technology is simple that no additional cost or complex control is needed. It can be expanded to any number of phases.

This paper is organized as follows. The current sharing performance of conventional multiphase *LLC* resonant converter is given in Section II. Section III discusses current sharing analysis of the proposed common inductor *LLC* resonant converter. The simulation results are provided in Section IV. Section V provides the experimental results of a two-phase 600-W *LLC* resonant converter prototype with both the conventional method and the proposed method. The paper is concluded in Section VI.

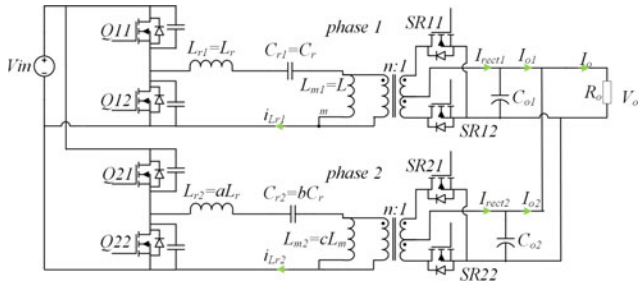

Fig. 5. Conventional two-phase *LLC* resonant converter.

II. Current Sharing Performance of Conventional Multiphase *LLC*

In this section, the current sharing performance of conventional multiphase *LLC* converter will be demonstrated. The FHA-based method introduced in [34] and [35] is used in this paper for analyzing the current sharing performance. This method utilizes the fact that the reflected ac voltages in the FHA method have the same magnitude for different phases [22], [32], [33] for equation solving. The highlight of the method is that it reveals that there exists a small phase difference between the reflected ac voltages. This method could be applied to both decoupled resonant tank (conventional structure) analysis and coupled resonant tank (common inductor structure) analysis.

A conventional two-phase *LLC* converter is shown in Fig. 5. Switches Q11, Q12, Q21, and Q22 are the primary HB switches of two phases. SR11, SR12, SR21, and SR22 are synchronous rectifiers on the secondary side of two phases.

L_{r1}, C_{r1}, and L_{m1} are the series inductor, series capacitor, and magnetizing inductor of phase 1. L_{r2}, C_{r2}, and L_{m2} are the series inductor, series capacitor, and magnetizing inductor of phase 2. i_{Lr1}, i_{Lr2}, I_{rect1}, I_{rect2}, I_{o1}, I_{o2}, C_{o1}, and C_{o2} are the resonant current, rectifier current, load current, and output capacitor of two phases, respectively. *n* is transformer turn ratio. Parameters *a*, *b,* and *c* are used to indicate that the resonant parameters for these two phases are different. The parameter relationship between the two resonant tank is

$$\begin{cases} L_{r2} = aL_{r1} \\ C_{r2} = bC_{r1} \\ L_{m2} = cL_{m1} \end{cases}. \tag{1}$$

To evaluate the current sharing performance, the load current sharing error σ_{load} is defined in (2), where I_{o1} and I_{o2} are the dc value of output current for the two phases. For space consideration, the detailed derivation process will not be presented in this paper. The load sharing error can be calculated using the method in [34] and [35] with given tolerance combination *a*, *b,* and *c*

$$\sigma_{\mathrm{load}} = \mathrm{abs}\left(\frac{I_{o1} - I_{o2}}{I_{o1} + I_{o2}}\right). \tag{2}$$

To analyze the current sharing performance, a set of *LLC* parameters, based on load power 300 W of each phase, is designed as shown in Table I using the existing design method [36].

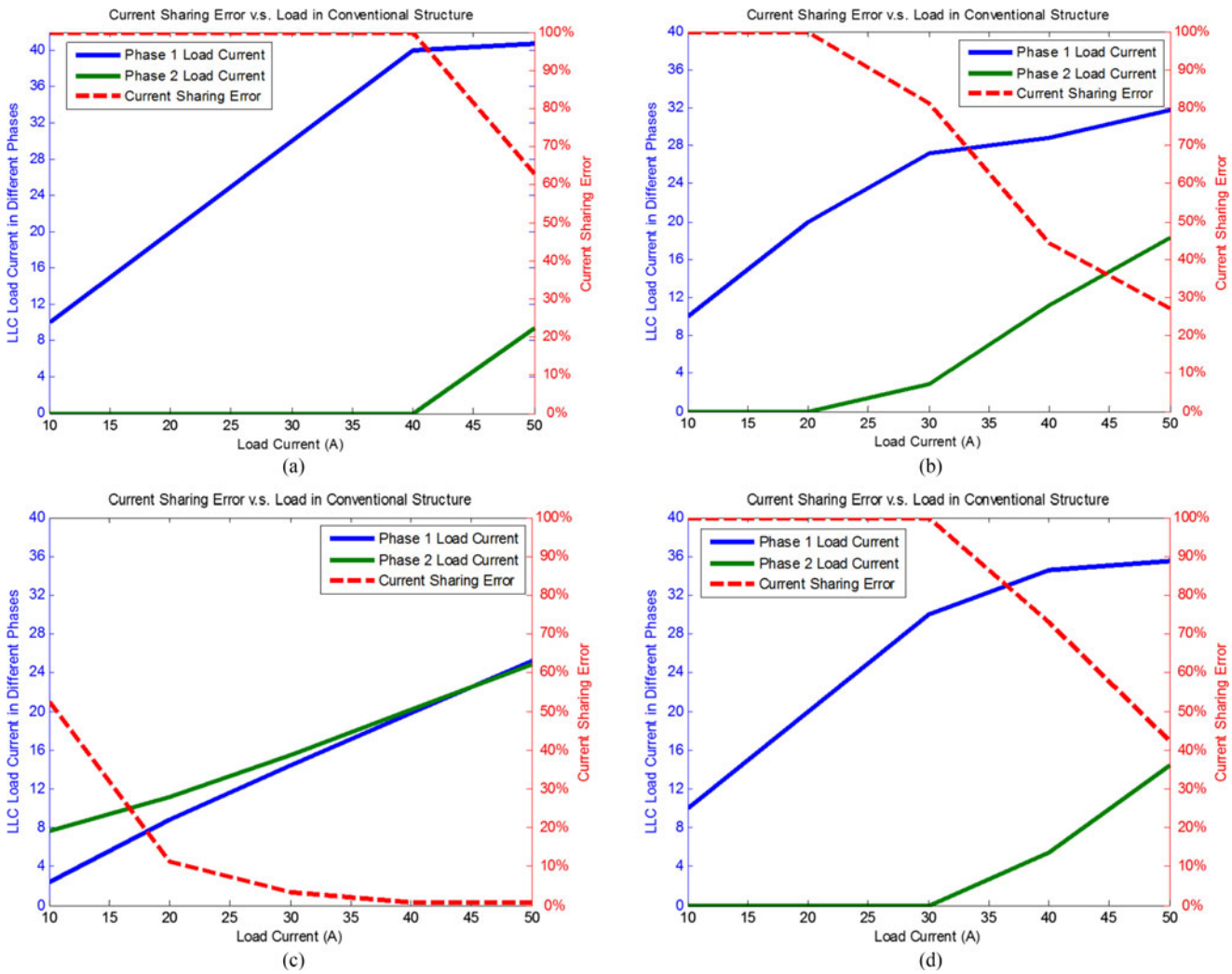

Fig. 6. Load current sharing error of conventional *LLC* converter at 400 V input and different component tolerance. (a) $L_{r2} = 1.05\,L_{r1}$, $C_{r2} = 1.05\,C_{r1}$, and $L_{m2} = 1.05\,L_{m1}$. (b) $L_{r2} = 0.95\,L_{r1}$, $C_{r2} = 1.05\,C_{r1}$, and $L_{m2} = 1.05\,L_{m1}$. (c) $L_{r2} = 1.05\,L_{r1}$, $C_{r2} = 0.95\,C_{r1}$, and $L_{m2} = 1.05\,L_{m1}$. (d) $L_{r2} = 1.05\,L_{r1}$, $C_{r2} = 1.05\,C_{r1}$, and $L_{m2} = 0.95\,L_{m1}$.

TABLE I
NOMINAL PARAMETER VALUE

Input voltage	340–400 V
Resonant inductor L_r	29 μH
Resonant capacitor C_r	12 nF
Magnetizing inductor L_m	95 μH
Transformer ratio n	20
Resonant frequency f_r	270 kHz
Output voltage V_o	12 V (rated voltage)
Total Output load P_o	full power 600 W
	half power 300 W

Fig. 6 shows load current sharing error σ_{load} of the conventional two-phase *LLC* converter at 400 V input with different component tolerances. The current sharing performance is evaluated at $\pm 5\%$ component tolerances. In the case $L_{r2} = L_{r1}$, $C_{r2} = C_{r1}$, and $L_{m2} = L_{m1}$, the two phases have the same parameters, which will result in the load current be perfectly shared, i.e., $\sigma_{\text{load}} = 0$. If $L_{r2} = 1.05\,L_{r1}$, $C_{r2} = 1.05\,C_{r1}$, and $L_{m2} = 1.05\,L_{m1}$, it means that the resonant component values of resonant inductance, resonant capacitance, and magnetizing inductance in phase #2 are all 5% more than the values in phase #1, respectively.

Theoretically, there are total eight (2^3) possible combinations for L_r, C_r, and L_m at $\pm 5\%$ tolerance. In terms of performance, four of the total eight combinations are just equivalent to the other four types—current sharing error is same, while current distribution is opposite. For example, the case $L_{r2} = 1.05\,L_{r1}$, $C_{r2} = 1.05\,C_{r1}$, and $L_{m2} = 1.05\,L_{m1}$ is equivalent to the case $L_{r2} = 0.95\,L_{r1}$, $C_{r2} = 0.95\,C_{r1}$, and $L_{m2} = 0.95\,L_{m1}$. If under the case $L_{r2} = 1.05\,L_{r1}$, $C_{r2} = 1.05\,C_{r1}$, and $L_{m2} = 1.05\,L_{m1}$, phase #1 provides 40 A of total 50 A, while phase #2 provides the rest 10 A, then the difference is 30 A and the current sharing error is 60%. Then, approximately for the case $L_{r2} = 0.95\,L_{r1}$, $C_{r2} = 0.95\,C_{r1}$, and $L_{m2} = 0.95\,L_{m1}$, phase #1 will provide 10 A of total 50 A, and phase #2 provides the rest 40 A, then the current sharing error will still be 60%. Thus, from the point of view of current sharing error, the four cases studied in Fig. 6 have covered all possible cases at 5% tolerance level.

Fig. 6(a) shows the load currents of two phases and load current sharing error, where $L_{r2} = 1.05\,L_{r1}$, $C_{r2} = 1.05\,C_{r1}$,

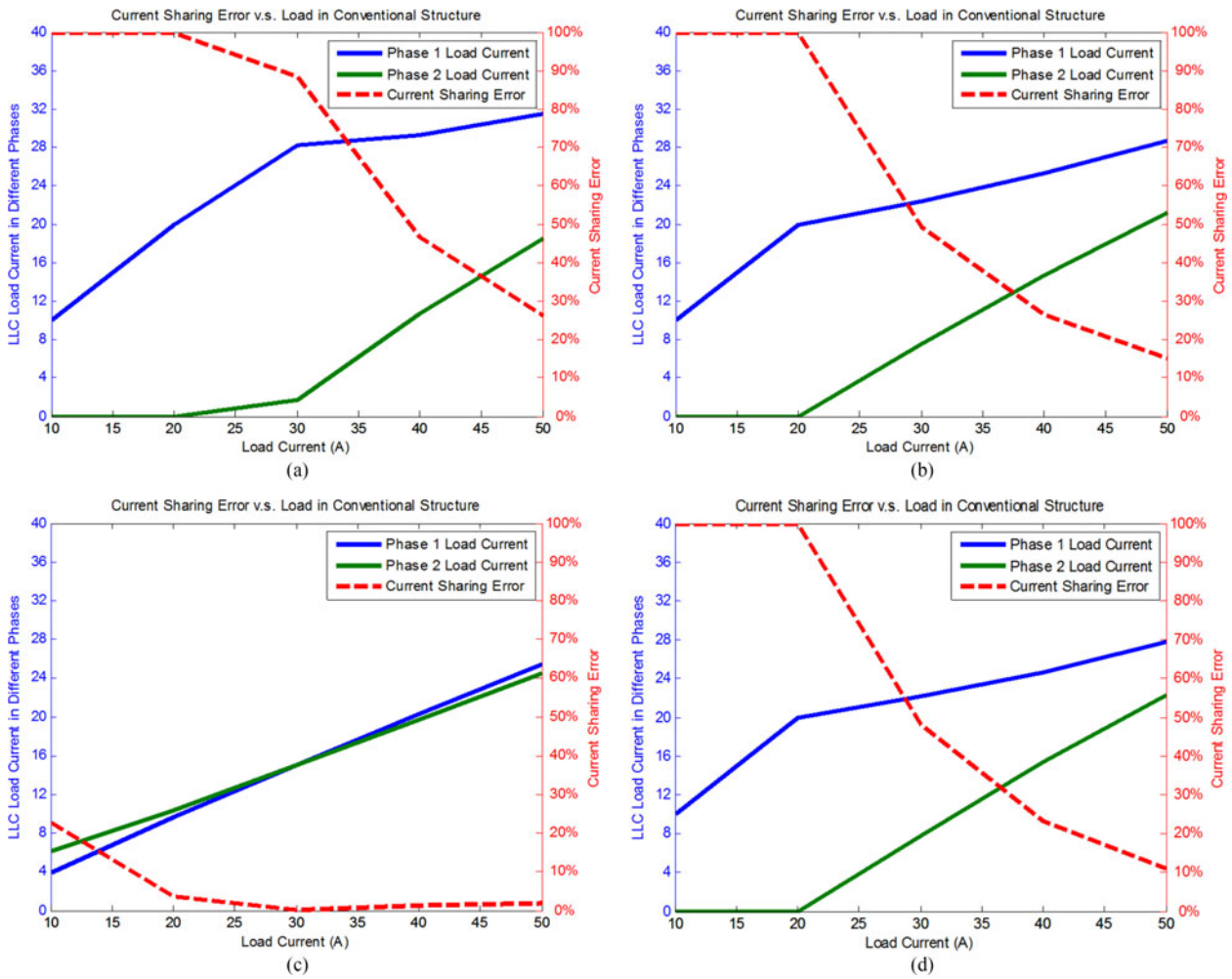

Fig. 7. Load current sharing error of conventional *LLC* converter at 340 V input and different component tolerance. (a) $L_{r2} = 1.05\,L_{r1}$, $C_{r2} = 1.05\,C_{r1}$, and $L_{m2} = 1.05\,L_{m1}$. (b) $L_{r2} = 0.95\,L_{r1}$, $C_{r2} = 1.05\,C_{r1}$, and $L_{m2} = 1.05\,L_{m1}$. (c) $L_{r2} = 1.05\,L_{r1}$, $C_{r2} = 0.95\,C_{r1}$, and $L_{m2} = 1.05\,L_{m1}$. (d) $L_{r2} = 1.05\,L_{r1}$, $C_{r2} = 0.95\,C_{r1}$, and $L_{m2} = 1.05\,L_{m1}$.

and $L_{m2} = 1.05\,L_{m1}$. The tolerances of resonant inductor and resonant capacitor are in the same direction (both > 1), then the resonant frequency of phase 2 deviates from that of phase 1, thus, the current sharing error is large. When the total load current is smaller than 40 A, only phase 1 provides the total load power, and the load current sharing error is 100%. When the total load current is 50 A, phase 1 will provide 41 A, and phase 2 will provide only 9 A.

Fig. 6(b) shows the load currents of two phases and the load current sharing error, where $L_{r2} = 0.95\,L_{r1}$, $C_{r2} = 1.05\,C_{r1}$, and $L_{m2} = 1.05\,L_{m1}$. The tolerance of resonant inductor is smaller than 1, and the tolerance of resonant capacitance is larger than 1. Thus, the resonant frequency of phase 2 is almost same with phase 1. If the total load current is smaller than 20 A, only phase 1 provides the total load power. Load current of phase 1 is 32 A when the total load current is 50 A.

Fig. 6(c) shows the load currents of two phases and the load current sharing error, where $L_{r2} = 1.05\,L_{r1}$, $C_{r2} = 0.95\,C_{r1}$, and $L_{m2} = 1.05\,L_{m1}$. The resonant frequency of phase 2 is almost same with phase 1 because the tolerance of resonant inductance is larger than 1 and the tolerance of resonant capacitance is smaller than 1. Good current sharing performance can be achieved—the current sharing error is smaller than 3% when the total load current is larger than 30 A. The maximum load current of phase 2 is about 25.3 A at 50 A total load current.

In Fig. 6(d), $L_{r2} = 1.05\,L_{r1}$, $C_{r2} = 1.05\,C_{r1}$, and $L_{m2} = 0.95\,L_{m1}$. The tolerances of resonant inductor and resonant capacitor is in the same direction (both > 1), then the resonant frequency of phase 2 deviates from that of phase 1, thus, the current sharing error is large. When the total load current is smaller than 30 A, only phase 1 provides the total load power, and the load current sharing error is 100%. Load current of phase 1 is 36 A when the total load current is 50 A.

Thus, the worst case is working under $L_{r2} = 1.05\,L_{r1}$, $C_{r2} = 1.05\,C_{r1}$, and $L_{m2} = 1.05\,L_{m1}$, as shown in Fig. 6(a). The conventional two-phase converter cannot share the load current for most load cases. In practice, if the two phases cannot achieve current sharing, then each phase has to be designed for 50 A (600 W) rather than 25 A (300 W) from the safety point of view, which goes against the initial desire to use two-phase converter to reduce current stresses.

Fig. 7 shows the current sharing performance at 340 V input condition for conventional two-phase *LLC* converter with difference tolerance combinations.

In Fig. 7, it could be observed that generally better current sharing performance could be achieved at 340 V input condition as compared to 400 V case. For different tolerance combinations, the results for 340 V input condition are similar as compared to 400 V input results. The worst case happens when the three component tolerance is in the same direction, i.e., $L_{r2} = 1.05\,L_{r1}$, $C_{r2} = 1.05\,C_{r1}$, and $L_{m2} = 1.05\,L_{m1}$.

For the input voltage between 340 and 400 V, the current sharing performance is also in between, i.e., better than 400 V performance while worse than 340 V performance.

III. Current Sharing Characteristic of Common Inductor Multiphase *LLC* Converter

As shown in Fig. 5, the two *LLC* phases in conventional structure are connected in parallel at both the input side and the output side. Thus, the resonant tank of each phase is completely independent of the other phase. No current information can be exchanged between the phases, and no current sharing can be achieved.

From the voltage gain point of view, if the two phases provide the same load current, then the output voltage V_o will have certain discrepancy due to the components tolerances. In real case, the output of the two phases is connected together at the load side. This is equal to say, the V_o of the two phases is equal. In order to eliminate the discrepancy on the gain-to-control diagram, the phase with higher voltage gain will provide more load power so that the voltage gain will reduce, whereas the phase with lower voltage gain will provide less power, and the voltage gain will increase. This explains the unbalanced load current at the steady state of conventional two-phase *LLC* converter.

In this paper, a new multiphase *LLC* resonant converter is proposed. The resonant inductors of different phases are connected in parallel to form a common inductor branch, which will take in the current of each phase and then redistribute evenly. In the proposed common inductor *LLC* converter, the resonant inductor of the two phases is connected together, thus the tolerance on the resonant inductor is automatically removed. Besides, the common inductor could be equivalent to one virtual inductor plus one virtual resistor for each phase [34], [35]. The virtual resistor will always be positive for the phase with higher load current, and negative for the phase lower current. In this way, the positive virtual resistor will increase the input impedance and thus reduce the current for that phase, whereas the negative virtual resistor will increase the current for the other phase. As a result, the two phases will have the same load current.

For easy understanding, a two-phase common inductor *LLC* resonant converter will be discussed in this section. Current sharing performance will be evaluated through FHA analysis.

A. Common Inductor Two-Phase LLC Resonant Converter

Fig. 8 shows the proposed two-phase common inductor *LLC* resonant converter. The series resonant inductors of the two *LLC* converters are connected in parallel.

It can also be implemented with one inductor whose value equals to the total inductance of L_{r1} and L_{r2} in parallel. *a, b,* and *c* are the component tolerances of phase 2 as compared to phase 1. For simplicity, Q11 and Q21 have same drive signal. Q12 and Q22 have same drive signal.

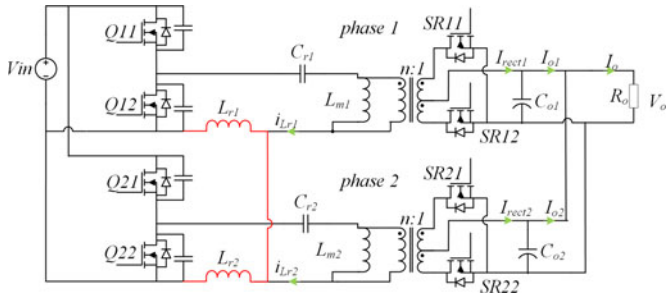

Fig. 8. Common inductor two-phase *LLC* resonant converter.

In Fig. 8, V_o, P_o, and R_o are the output voltage, total output power, and total load resistor of the two phases. The load resistor can be expressed as follows:

$$R_o = \frac{{V_o}^2}{P_o}. \tag{3}$$

In steady state, the total load power P_o is separated into P_{o1} for phase 1 and P_{o2} for phase 2 as

$$P_o = P_{o1} + P_{o2}. \tag{4}$$

The equivalent load resistors of each phase are R_{o1} and R_{o2} as

$$\begin{cases} R_{o1} = \frac{{V_o}^2}{P_{o1}} \\ R_{o2} = \frac{{V_o}^2}{P_{o2}} \end{cases}. \tag{5}$$

The coefficient *k* is defined as the phase 1 load power proportion of total load power. Then, the load power P_{o1} of phase 1 and P_{o2} of phase 2 can be expressed as

$$P_{o1} = kP_o \tag{6}$$

$$P_{o2} = (1-k)P_o. \tag{7}$$

Combining (3)–(7) gives

$$\left[R_{o1}\ R_{o2}\right] = \begin{cases} \left[\infty\ R_o\right], & k = 0 \\ \left[R_o/_k\ R_o/_{1-k}\right], & k \in (0,1) \\ \left[R_o\ \infty\right], & k = 1 \end{cases}. \tag{8}$$

B. Current Sharing Analysis of the Proposed Two-Phase LLC Resonant Converter

Mathematical model of the *LLC* converter is needed for analyzing the current sharing performance of the two-phase *LLC* converter. FHA circuit is used to analyze the two-phase *LLC* resonant converter [34], [35], in which the resonant tanks of each phase are coupled. The equivalent circuit is shown in Fig. 9. According to (1), the total resonant inductance L_{r_total} is

$$L_{r\_\mathrm{total}} = \frac{a}{1+a}L_r. \tag{9}$$

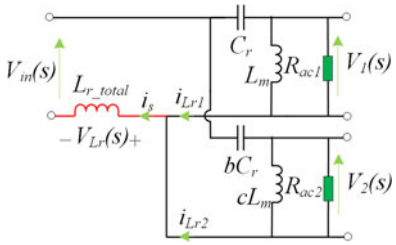

Fig. 9. FHA equivalent circuit of the proposed two-phase *LLC* resonant converter.

The primary-side equivalent ac resistors R_{ac1} and R_{ac2} are

$$\begin{cases} R_{\mathrm{ac1}} = \frac{8n^2}{\pi^2} R_{o1} \\ R_{\mathrm{ac2}} = \frac{8n^2}{\pi^2} R_{o2} \end{cases}. \tag{10}$$

Combing (8) and (10) gives

$$\begin{bmatrix} R_{\mathrm{ac1}} & R_{\mathrm{ac2}} \end{bmatrix} = \begin{cases} \begin{bmatrix} \infty & \frac{8n^2}{\pi^2} R_o \end{bmatrix}, & k = 0 \\ \begin{bmatrix} \frac{8n^2 R_o}{\pi^2 k} & \frac{8n^2 R_o}{\pi^2 (1-k)} \end{bmatrix}, & k \in (0,1) \\ \begin{bmatrix} \frac{8n^2}{\pi^2} R_o & \infty \end{bmatrix}, & k = 1 \end{cases}. \tag{11}$$

In a steady-state operation, the voltage gains of each phase are same as they are connected to the same input voltage and output voltage. Thus, the magnitude of ac voltage $V_1(s)$ and $V_2(s)$ is the same, while the phase angles are always different due to parameter tolerance. The relationship is as follows:

$$|V_1(s)| = |V_2(s)|. \tag{12}$$

From Fig. 9, the transfer function of ac voltage $V_1(s)$ and $V_2(s)$ is

$$\begin{cases} V_1(s) = \frac{R_{\mathrm{ac1}} // sL_m}{R_{\mathrm{ac1}} // sL_m + 1/sC_r} (V_{\mathrm{in}}(s) + V_{\mathrm{Lr}}(s)) \\ V_2(s) = \frac{R_{\mathrm{ac2}} // scL_m}{R_{\mathrm{ac2}} // scL_m + 1/sbC_r} (V_{\mathrm{in}}(s) + V_{\mathrm{Lr}}(s)) \end{cases}. \tag{13}$$

Manipulating (10), (12), and (13), the load factor k can be calculated as

$$Ak^2 + Bk + C = 0. \tag{14}$$

For common inductor *LLC* converter, the coefficients *A, B*, and *C* for the proposed two-phase *LLC* converter are

$$\begin{cases} A = \omega^2 (1 - b^2) c^2 {L_m}^2 \\ B = -2\omega^2 c^2 {L_m}^2 \\ C = \omega^2 c^2 {L_m}^2 + (1 - b^2 c^2) {R_{\mathrm{ac}}}^2 - 2\omega^2 (bc - b^2 c^2) L_m C_r {R_{\mathrm{ac}}}^2 \end{cases}. \tag{15}$$

Combing (14) and (15), the load factor k can be solved for given input voltage and different load conditions. The load factor k is valid when k is between 0 and 1. Conditions $k = 0$ and $k = 1$ mean that only one phase provides all the power and the other phase does not provide power. $k < 0$ and $k > 1$ are invalid answers.

To evaluate the current sharing performance, the load current sharing error σ_{load} is defined as follows, where I_{o1} and I_{o2} are the dc value of output current for the two phases

$$\sigma_{\mathrm{load}} = \mathrm{abs}\left(\frac{I_{o1} - I_{o2}}{I_{o1} + I_{o2}}\right) = \mathrm{abs}(1 - 2k), \quad k \in [0,1]. \tag{16}$$

Similarly, the resonant current sharing error $\sigma_{\mathrm{Resonant}}$ is defined as follows, where $\mathrm{rms}(i_{\mathrm{Lr1}})$ and $\mathrm{rms}(i_{\mathrm{Lr2}})$ are the root-mean-square (rms) value of resonant current i_{Lr1} and i_{Lr2}:

$$\sigma_{\mathrm{Resonant}} = \mathrm{abs}\left(\frac{\mathrm{rms}(i_{\mathrm{Lr1}}) - \mathrm{rms}(i_{\mathrm{Lr2}})}{\mathrm{rms}(i_{\mathrm{Lr1}}) + \mathrm{rms}(i_{\mathrm{Lr2}})}\right). \tag{17}$$

When N ($N > 2$) phases are connected in parallel, the load current sharing error and resonant current sharing error are defined as follows, where, N is the phase number, $\mathrm{rms}(i_{\mathrm{Lrj}})$ and I_{oj} are resonant current rms value and output current of the jth phase:

$$\begin{cases} \sigma_{\mathrm{load}-j} = \mathrm{abs}\left[\frac{I_{0j} - \sum_{j=1}^{N} I_{0j}/N}{\sum_{j=1}^{N} I_{0j}/N}\right] \\ \sigma_{\mathrm{Resonant}-j} = \mathrm{abs}\left[\frac{\mathrm{rms}(i_{\mathrm{Lrj}}) - \sum_{j=1}^{N} \mathrm{rms}(i_{\mathrm{Lrj}})/N}{\sum_{j=1}^{N} \mathrm{rms}(i_{\mathrm{Lrj}})/N}\right] \end{cases}. \tag{18}$$

C. Current Sharing Performance With Specific Parameters

In this section, current sharing performance will be demonstrated with specific *LLC* parameters. The parameters of phase 1 have been given in Table I.

Fig. 10 shows load current sharing error σ_{load} of the proposed two-phase *LLC* converter at 400 V input condition under different component tolerances. The $\pm 5\%$ component tolerance is assumed to evaluate the current sharing performance.

Fig. 10(a) shows the load currents of two phases and load current sharing error, where $L_{r2} = 1.05\,L_{r1}$, $C_{r2} = 1.05\,C_{r1}$, and $L_{m2} = 1.05\,L_{m1}$. The load current sharing error is 6% at 50 A total load. The maximum current of phase 1 is 26.5 A and the maximum current of phase 2 is 23.5 A when the total load current is 50 A. The good current sharing performance can be achieved with total load current increasing.

Fig. 10(b) shows the load currents of two phases and the load current sharing error where $L_{r2} = 0.95\,L_{r1}$, $C_{r2} = 1.05\,C_{r1}$, and $L_{m2} = 1.05\,L_{m1}$. Almost same current sharing performance can be achieved in both Fig. 10(a) and (b) as the tolerance of resonant inductance does not impact the current sharing error because of in parallel of each resonant inductors based on proposed multiphase *LLC* resonant converter. The maximum load currents of each phase are 26.5 and 23.5 A under total 50 A load. The current sharing error is about 6%.

Fig. 10(c) shows the load currents of two phases and the load current sharing error where $L_{r2} = 1.05\,L_{r1}$, $C_{r2} = 0.95\,C_{r1}$, and $L_{m2} = 1.05\,L_{m1}$. The current sharing performance can be achieved from light load to heavy load. The maximum load current of two phases is 25.5 and 24.5 A under total 50 A load. The current sharing error is about 2%. The load currents are almost same for each phase.

Fig. 10(d) shows the load currents of two phases and the load current sharing error where $L_{r2} = 1.05\,L_{r1}$, $C_{r2} = 1.05\,C_{r1}$ and $L_{m2} = 0.95\,L_{m1}$. The current sharing performance can be achieved from light load to heavy load. The maximum load currents of each phase are 25.7 and 24.3 A under total 50 A

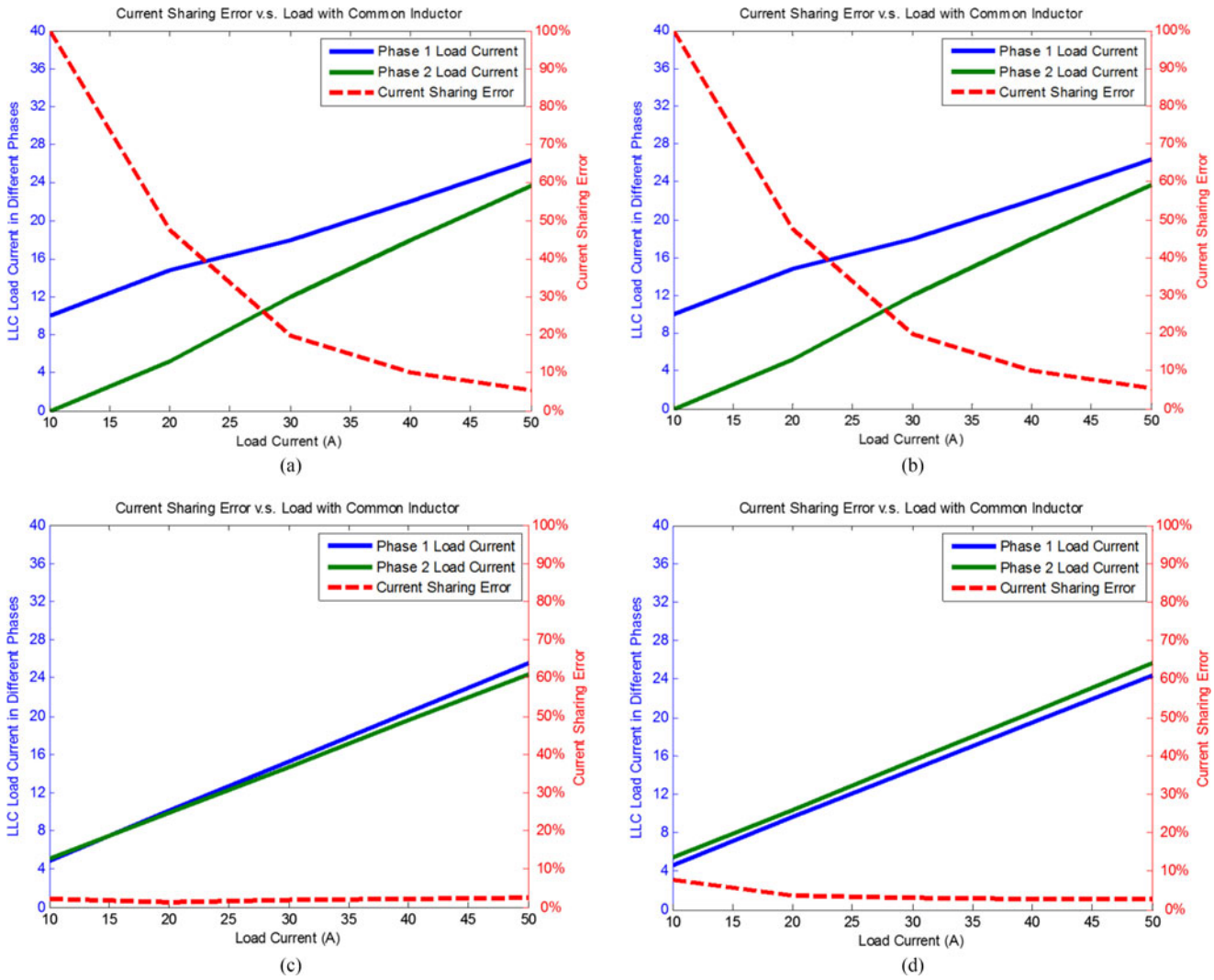

Fig. 10. Load current sharing error of common inductor *LLC* converter at 400 V input and different component tolerance. (a) $L_{r2} = 1.05\,L_{r1}$, $C_{r2} = 1.05\,C_{r1}$, and $L_{m2} = 1.05\,L_{m1}$. (b) $L_{r2} = 0.95\,L_{r1}$, $C_{r2} = 1.05\,C_{r1}$, and $L_{m2} = 1.05\,L_{m1}$. (c) $L_{r2} = 1.05\,L_{r1}$, $C_{r2} = 0.95\,C_{r1}$, and $L_{m2} = 1.05\,L_{m1}$. (d) $L_{r2} = 1.05\,L_{r1}$, $C_{r2} = 1.05\,C_{r1}$, and $L_{m2} = 0.95\,L_{m1}$.

load. The current sharing error is about 2.8%.The load current is almost same for each phase.

Comparing the four tolerance combinations, it could be concluded that the worst case is under $L_{r2} = 1.05\,L_{r1}$, $C_{r2} = 0.95\,C_{r1}$, and $L_{m2} = 1.05\,L_{m1}$, as shown in–Fig. 10(a). Still, good current sharing performance (6% current sharing error) can also be achieved.

Fig. 11 shows the current sharing performance at 340 V input voltage condition for common inductor *LLC* converter with difference tolerance combinations.

From Fig. 11, it could be observed that the current sharing performance at 340 V input condition is very similar with that at 400 V input. As the tolerance on the resonant inductor L_r has been eliminated, the results for case (a) are basically the same with case (b). Same result can be found on case (c) and case (d). The worst case happens when the resonant capacitor C_r deviates to the same direction with the magnetizing inductor L_m.

For input voltage between 340 and 400 V, the current sharing performance is in between and very similar.

IV. Simulation Results

In order to verify and compare the current sharing performance further, in this section, PSIM simulation results of both conventional two-phase *LLC* converter and the proposed common inductor *LLC* converter will be provided.

In Sections IV-A and IV-B, for respective 400 and 340 V input voltage condition, PSIM simulation results will be compared to FHA calculation for both conventional structure and proposed common inductor structure at ±5% tolerances level. Four types of tolerance combination will be included:

1) $L_{r2} = 1.05\,L_{r1}$, $C_{r2} = 1.05\,C_{r1}$, and $L_{m2} = 1.05\,L_{m1}$ tolerance;
2) $L_{r2} = 0.95\,L_{r1}$, $C_{r2} = 1.05\,C_{r1}$, and $L_{m2} = 1.05\,L_{m1}$ tolerance;
3) $L_{r2} = 1.05\,L_{r1}$, $C_{r2} = 0.95\,C_{r1}$, and $L_{m2} = 1.05\,L_{m1}$ tolerance;
4) $L_{r2} = 1.05\,L_{r1}$, $C_{r2} = 1.05\,C_{r1}$, and $L_{m2} = 0.95\,L_{m1}$ tolerance.

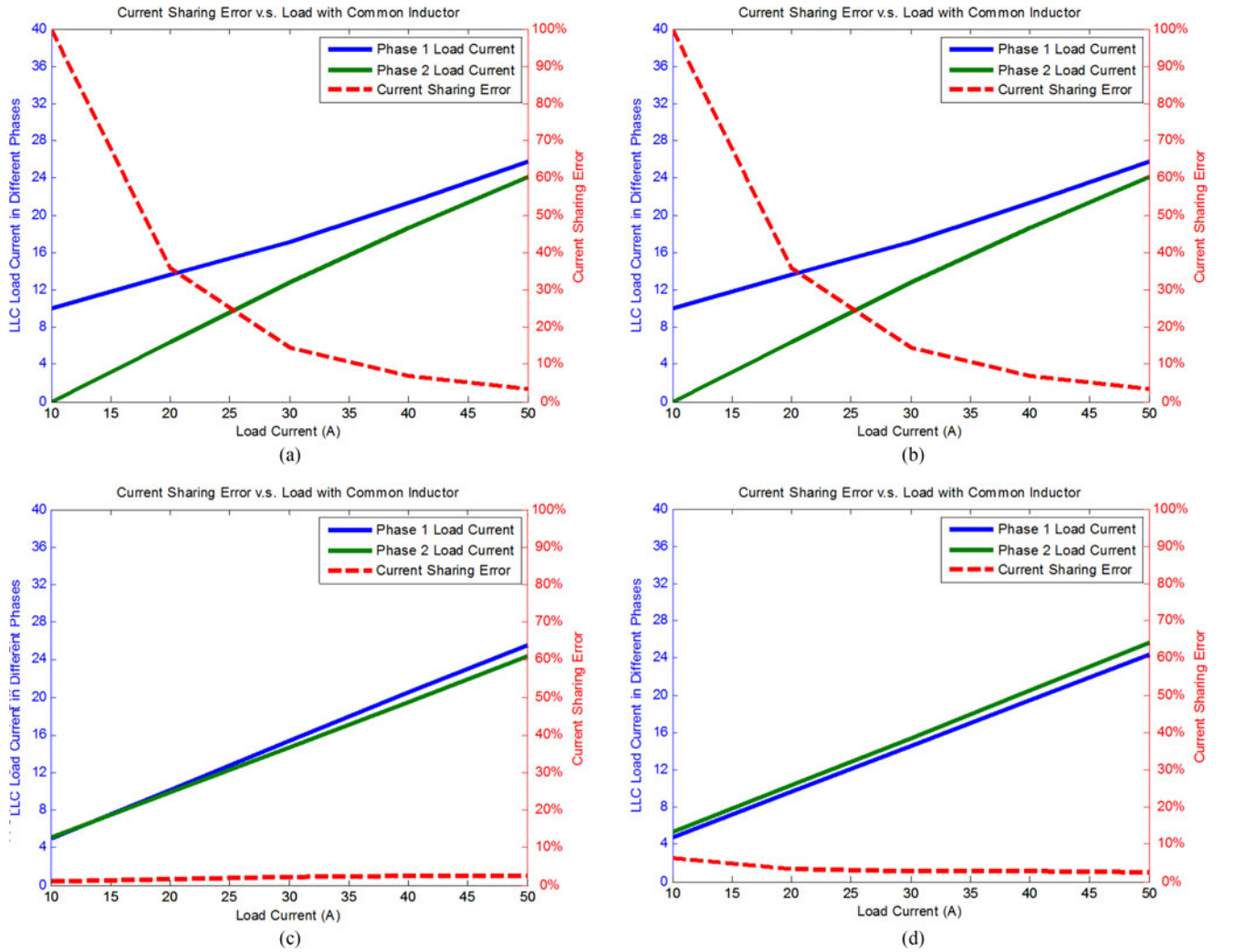

Fig. 11. Load current sharing error of common inductor *LLC* converter at 340 V input and different component tolerance. (a) $L_{r2} = 1.05\,L_{r1}$, $C_{r2} = 1.05\,C_{r1}$, and $L_{m2} = 1.05\,L_{m1}$. (b) $L_{r2} = 0.95\,L_{r1}$, $C_{r2} = 1.05\,C_{r1}$, and $L_{m2} = 1.05\,L_{m1}$. (c) $L_{r2} = 1.05\,L_{r1}$, $C_{r2} = 0.95\,C_{r1}$, and $L_{m2} = 1.05\,L_{m1}$. (d) $L_{r2} = 1.05\,L_{r1}$, $C_{r2} = 1.05\,C_{r1}$, and $L_{m2} = 0.95\,L_{m1}$.

In Section IV-C, the deviation between FHA and PSIM results will be explained.

In Section IV-D, simulation waveforms based on the measured prototype parameters will be shown at different load current. The leakage inductor of transformers will also be considered in the simulation.

A. Two-Phase LLC Simulation Results Under 400 V With Different Tolerance Combinations

The simulation is conducted under 400 V input and total 50 A load condition. The rated output voltage is 12 V. The parameters of two phases are shown in Table II.

Fig. 12 shows the PSIM simulation waveforms of the resonant current, rectifier current of conventional two-phase *LLC* converter at 400 V input voltage condition.

Table III shows the load current ($I_{\mathrm{rect1\_}ave}$ and $I_{\mathrm{rect2\_}ave}$) of FHA calculation and PSIM simulation. It can be observed that load current sharing error σ_{load} from simulation matches with the calculation results in general trends (the value is different).

TABLE II
PARAMETERS OF TWO-PHASE *LLC* CONVERTER IN PSIM

	Resonant Inductor L_r	Resonant capacitor C_r	Magnetizing inductor L_m
Phase 1 (reference)	29 μH	12 nF	95 μH
Phase 2 (a)	30.5 μH (+5%)	12.6 nF (+5%)	100 μH (+5%)
Phase 2 (b)	28.5 μH (–5%)	12.6 nF (+5%)	100 μH (+5%)
Phase 2 (c)	30.5 μH (+5%)	11.4 nF (–5%)	100 μH (+5%)
Phase 2 (d)	30.5 μH (+5%)	12.6 nF (+5%)	90 μH (–5%)

The difference is generally caused by the absence of high-order harmonics in FHA. In PSIM simulation, the worst case $L_{r2} = 1.05\,L_{r1}$, $C_{r2} = 1.05\,C_{r1}$, and $L_{m2} = 1.05\,L_{m1}$ of load current sharing error σ_{load} reaches 98%, and almost only phase #1 provides the total 50 A load current.

Fig. 13 shows the PSIM simulation waveforms of the resonant current and rectifier current of the common inductor two-phase *LLC* converter at 400 V input condition.

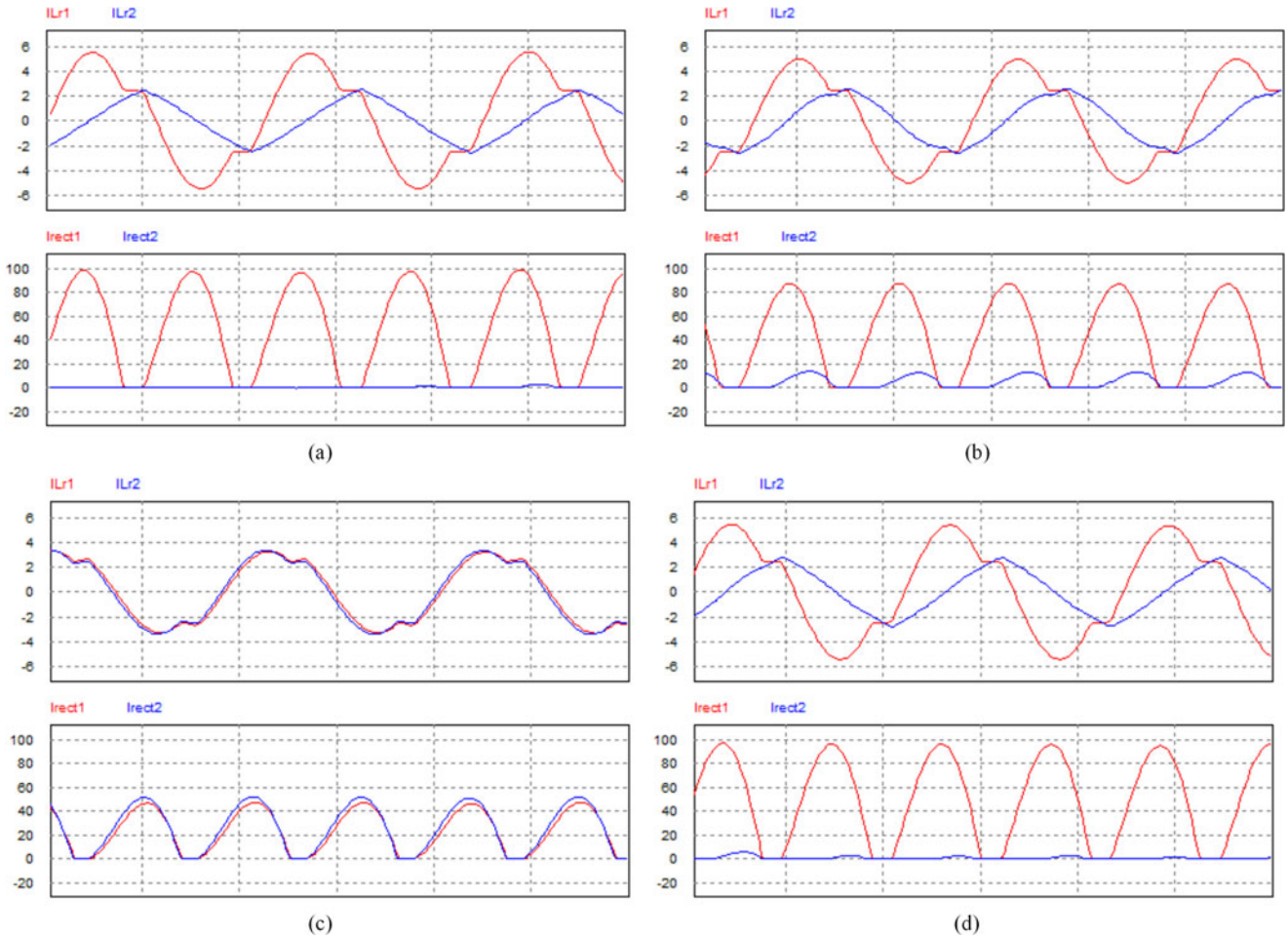

Fig. 12. Simulation results of conventional two-phase *LLC* converter with +5% tolerance at 400 V input condition. (a) $L_{r2} = 1.05\,L_{r1}$, $C_{r2} = 1.05\,C_{r1}$, and $L_{m2} = 1.05\,L_{m1}$. (b) $L_{r2} = 0.95\,L_{r1}$, $C_{r2} = 1.05\,C_{r1}$, and $L_{m2} = 1.05\,L_{m1}$. (c) $L_{r2} = 1.05\,L_{r1}$, $C_{r2} = 0.95\,C_{r1}$, and $L_{m2} = 1.05\,L_{m1}$. (d) $L_{r2} = 1.05\,L_{r1}$, $C_{r2} = 1.05\,C_{r1}$, and $L_{m2} = 0.95\,L_{m1}$.

TABLE III
DATA COMPARISON OF SIMULATION AND FHA CALCULATION OF CONVENTIONAL TWO-PHASE *LLC* CONVERTER AT 400 V INPUT CONDITION

Tolerances	FHA calculation			PSIM simulation		
	I_{rect1_ave}	I_{rect2_ave}	σ_{load_FHA}	I_{rect1_ave}	I_{rect2_ave}	σ_{load_PSIM}
Type a: (*a, b, c*) = (1.05, 1.05, 1.05)	41	9	64%	49.5	0.5	98%
Type b: (*a, b, c*) = (0.95, 1.05, 1.05)	32	18	28%	45	5	80%
Type c: (*a, b, c*) = (1.05, 0.95, 1.05)	24.5	25.5	2%	23.5	26.5	6%
Type d: (*a, b, c*) = (1.05, 1.05, 0.95)	36	14	44%	48	2	92%

In Fig. 13(a) and (b) when the tolerance on C_r (*b*) and the tolerance on L_m (*c*) deviates in the same direction, good current sharing performance could be achieved. In–Fig. 13(c) and (d), the two-phase current is almost the identical, which verifies the FHA calculation results in–Fig. 10(c) and (d).

Table IV shows the load current data comparison of FHA calculation and PSIM simulation for common inductor two-phase *LLC* converter at 400 V input condition.

The simulation results match well with the FHA prediction. At the worst case $L_{r2} = 1.05\,L_{r1}$, $C_{r2} = 1.05\,C_{r1}$, and $L_{m2} = 1.05\,L_{m1}$, the load current error between the two phases ($\sigma_{\rm load}$) is only 2%, while the worst case for conventional two-phase *LLC* is 98% (almost no sharing).

B. Two-Phase LLC Simulation Results Under 340 V With Different Tolerance Combinations

In real world, the converter will need to operate not only at 400 V (resonant frequency) but also at somewhere lower. As comparison, the 340 V 50A load operation results are also simulated. The parameters of two phases are shown in Table II.

Fig. 14 shows the simulation waveforms of conventional *LLC* converter for 340 V input.

The load current sharing error is summarized in Table V. It can be observed that the load current sharing error $\sigma_{\rm load}$ from simulation agrees with the calculation results in general trends (the value is different). In PSIM simulation, at the worst case $L_{r2} = 1.05\,L_{r1}$, $C_{r2} = 1.05\,C_{r1}$, and $L_{m2} = 1.05\,L_{m1}$,

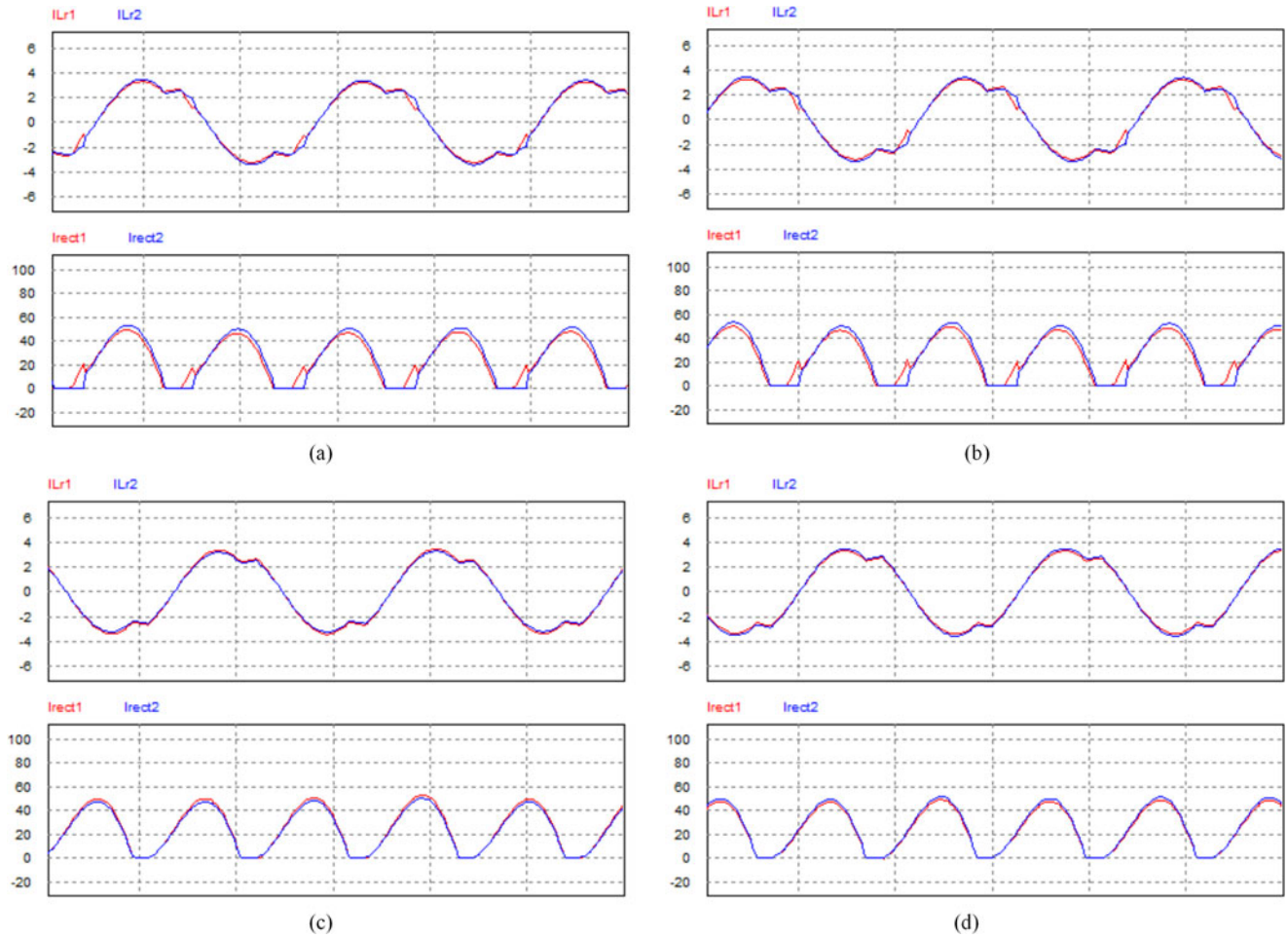

Fig. 13. Simulation results of common inductor two-phase *LLC* converter with +5% tolerance at 400 V input condition. (a) $L_{r2} = 1.05\,L_{r1}$, $C_{r2} = 1.05\,C_{r1}$, and $L_{m2} = 1.05\,L_{m1}$. (b) $L_{r2} = 0.95\,L_{r1}$, $C_{r2} = 1.05\,C_{r1}$, and $L_{m2} = 1.05\,L_{m1}$. (c) $L_{r2} = 1.05\,L_{r1}$, $C_{r2} = 0.95\,C_{r1}$, and $L_{m2} = 1.05\,L_{m1}$. (d) $L_{r2} = 1.05\,L_{r1}$, $C_{r2} = 1.05\,C_{r1}$, and $L_{m2} = 0.95\,L_{m1}$.

TABLE IV
DATA COMPARISON OF SIMULATION AND FHA CALCULATION OF COMMON INDUCTOR *LLC* CONVERTER AT 400 V INPUT CONDITION

Tolerances	FHA calculation			PSIM simulation		
	I_{rect1_ave}	I_{rect2_ave}	σ_{load_FHA}	I_{rect1_ave}	I_{rect2_ave}	σ_{load_PSIM}
Type a: (*a, b, c*) = (1.05, 1.05, 1.05)	26.5	23.5	6%	24.5	25.5	2%
Type b: (*a, b, c*) = (0.95, 1.05, 1.05)	26.5	23.5	6%	24.5	25.5	2%
Type c: (*a, b, c*) = (1.05, 0.95, 1.05)	25.5	24.5	2%	25.5	24.5	2%
Type d: (*a, b, c*) = (1.05, 1.05, 0.95)	25.7	24.3	2.8%	24.2	25.8	1.6%

TABLE V
DATA COMPARISON OF SIMULATION AND FHA CALCULATION OF CONVENTIONAL TWO-PHASE *LLC* CONVERTER AT 340 V INPUT CONDITION

Tolerances	FHA calculation			PSIM simulation		
	I_{rect1_ave}	I_{rect2_ave}	σ_{load_FHA}	I_{rect1_ave}	I_{rect2_ave}	σ_{load_PSIM}
Type a: (*a, b, c*) = (1.05, 1.05, 1.05)	31.5	18.5	26%	49.5	0.5	98%
Type b: (*a, b, c*) = (0.95, 1.05, 1.05)	29	21	16%	36	14	44%
Type c: (*a, b, c*) = (1.05, 0.95, 1.05)	25.5	24.5	2%	24.7	25.2	1%
Type d: (*a, b, c*) = (1.05, 1.05, 0.95)	28	22	12%	45	5	80%

the load current sharing error σ_{load} reaches 98%, and almost phase 1 provides the total load power.

Fig. 15 shows the PSIM simulation waveforms of the resonant current and rectifier current of the common inductor two-phase *LLC* converter at 340 V input condition. The results are very similar to the 400 V operation results. The conclusion for 400 V results can also be applied to the 340 V operation that very good current sharing is achieved for all tolerances cases.

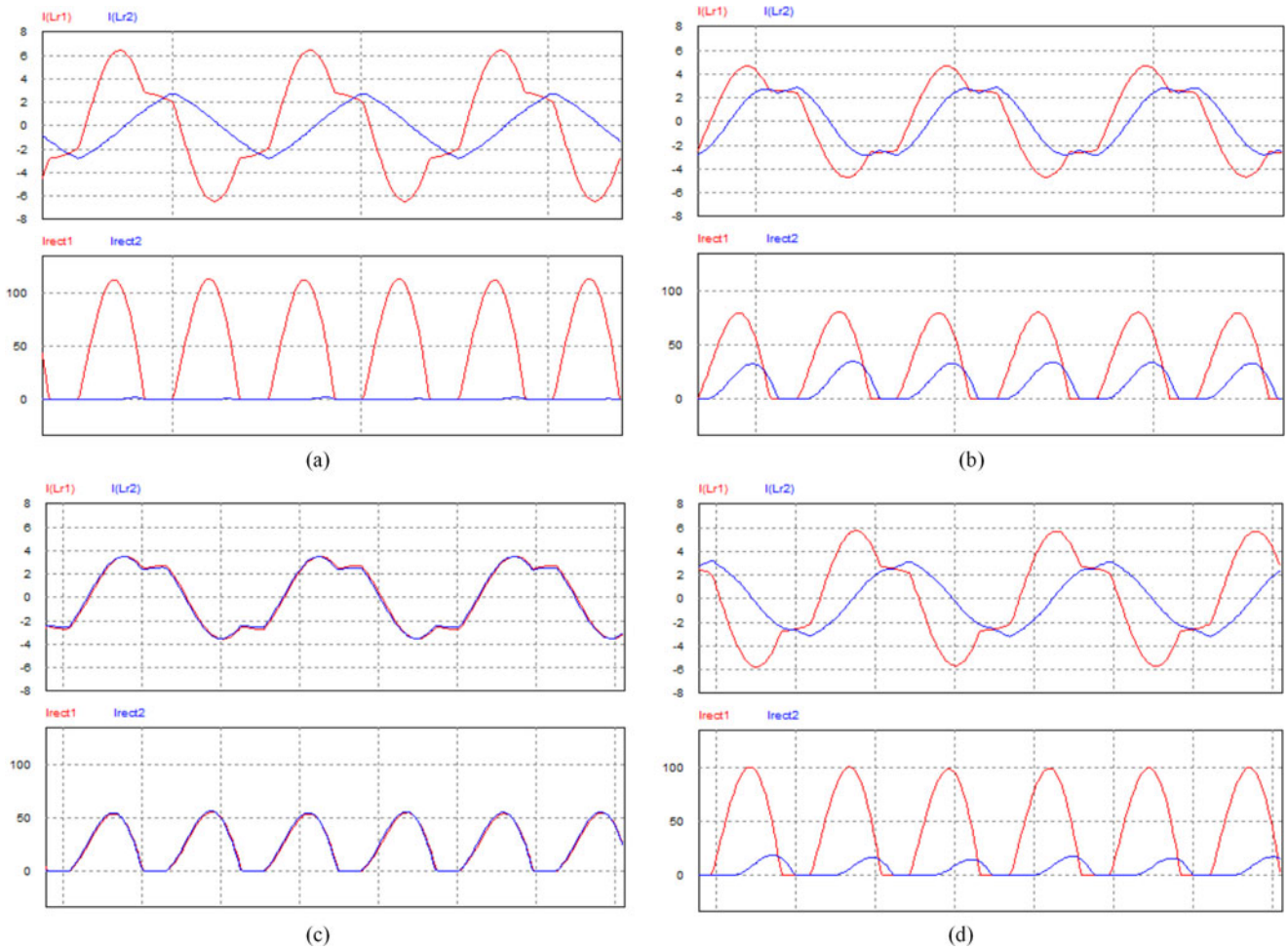

Fig. 14. Simulation results of conventional two-phase *LLC* converter with +5% tolerance at 340 V input condition. (a) $L_{r2} = 1.05\,L_{r1}$, $C_{r2} = 1.05\,C_{r1}$, and $L_{m2} = 1.05\,L_{m1}$. (b) $L_{r2} = 0.95\,L_{r1}$, $C_{r2} = 1.05\,C_{r1}$, and $L_{m2} = 1.05\,L_{m1}$. (c) $L_{r2} = 1.05\,L_{r1}$, $C_{r2} = 0.95\,C_{r1}$, and $L_{m2} = 1.05\,L_{m1}$. (d) $L_{r2} = 1.05\,L_{r1}$, $C_{r2} = 1.05\,C_{r1}$, and $L_{m2} = 0.95\,L_{m1}$.

TABLE VI
DATA COMPARISON OF SIMULATION AND FHA CALCULATION OF COMMON INDUCTOR *LLC* CONVERTER AT 340 V INPUT CONDITION

Tolerances	FHA calculation			PSIM simulation		
	I_{rect1_ave}	I_{rect2_ave}	σ_{load_FHA}	I_{rect1_ave}	I_{rect2_ave}	σ_{load_PSIM}
Type a: (*a, b, c*) = (1.05, 1.05, 1.05)	26	24	4%	24.3	25.7	2.8%
Type b: (*a, b, c*) = (0.95, 1.05, 1.05)	26	24	4%	24.3	25.7	2.8%
Type c: (*a, b, c*) = (1.05, 0.95, 1.05)	25.5	24.5	2%	25.5	24.5	2%
Type d: (*a, b, c*) = (1.05, 1.05, 0.95)	24.5	25.5	2%	24.4	25.6	2.4%

Table VI shows the load current data comparison of FHA calculation and PSIM simulation for common inductor two-phase *LLC* converter at 340 V input condition.

The simulation results match well with the FHA calculation. At the worst case $L_{r2} = 1.05\,L_{r1}$, $C_{r2} = 1.05\,C_{r1}$, and $L_{m2} = 1.05\,L_{m1}$, the load current error between the two phases (σ_{load}) is only 2.8%, while the worst case for conventional two-phase *LLC* is 98% (almost no sharing).

C. Error of FHA Analysis and PSIM Simulation

It is noted that computer simulation result by PSIM is more accurate than the FHA analysis. From Tables III and V, it is observed that the deviation between the PSIM result and the FHA analysis is larger for conventional two-phase *LLC* converter than that of the common inductor *LLC* converter shown in Tables IV and VI.

The deviation between PSIM simulation and FHA calculation is caused by the neglected high-order harmonics in FHA method. Therefore, at a given load current, the voltage gain calculated by FHA is lower than the actual case since only the fundamental harmonic is considered. Thus, in order to achieve the same output voltage, the switching frequency predicted by the FHA method is always lower than the actual switching frequency predicted by the PSIM simulation. In other words, the actual operating switching frequency will be higher than the switching frequency predicted by the FHA method.

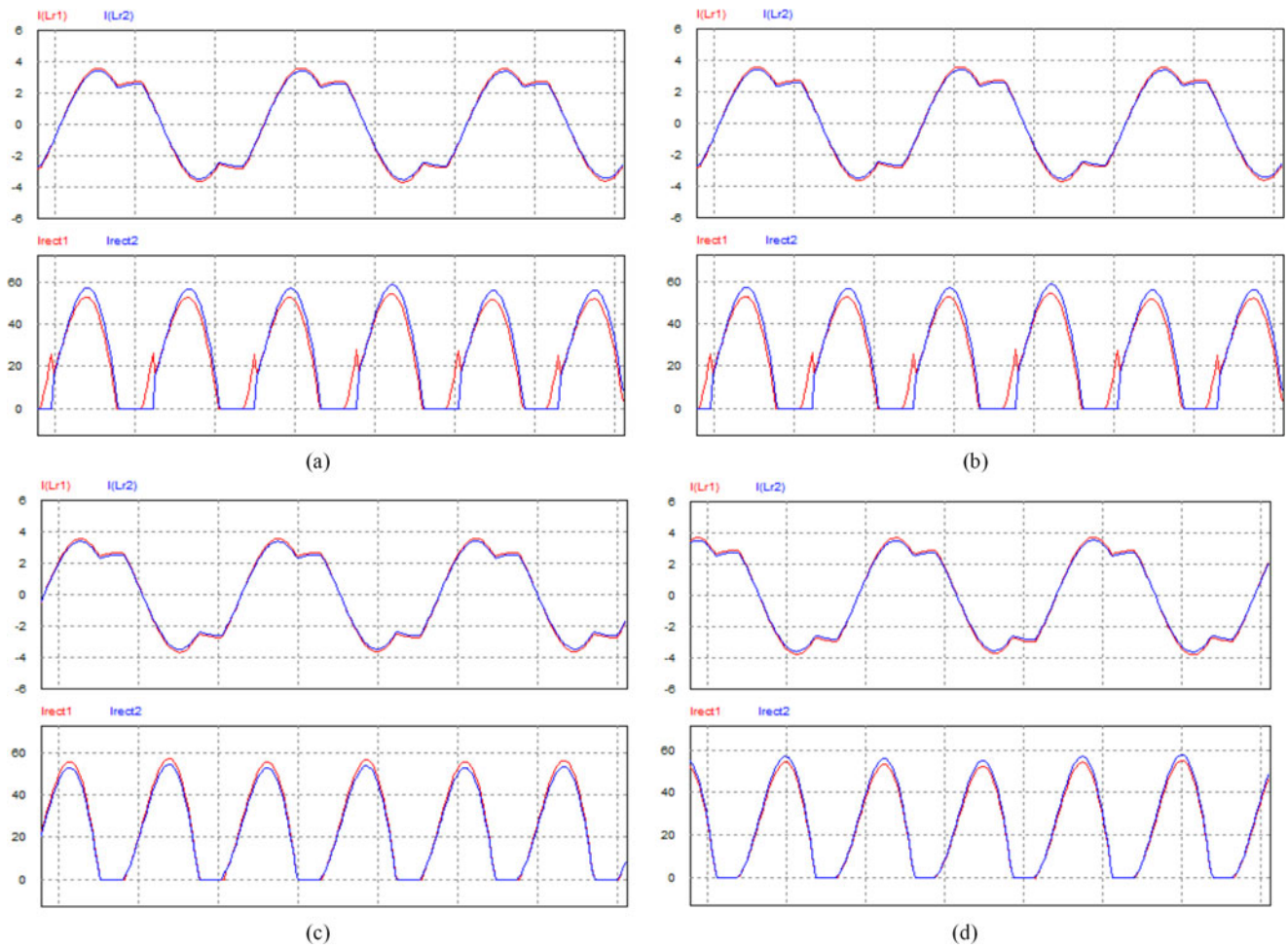

Fig. 15. Simulation results of common inductor two-phase *LLC* converter with +5% tolerance at 340 V input condition. (a) $L_{r2} = 1.05\,L_{r1}$, $C_{r2} = 1.05\,C_{r1}$, and $L_{m2} = 1.05\,L_{m1}$. (b) $L_{r2} = 0.95\,L_{r1}$, $C_{r2} = 1.05\,C_{r1}$, and $L_{m2} = 1.05\,L_{m1}$. (c) $L_{r2} = 1.05\,L_{r1}$, $C_{r2} = 0.95\,C_{r1}$, and $L_{m2} = 1.05\,L_{m1}$. (d) $L_{r2} = 1.05\,L_{r1}$, $C_{r2} = 1.05\,C_{r1}$, and $L_{m2} = 0.95\,L_{m1}$.

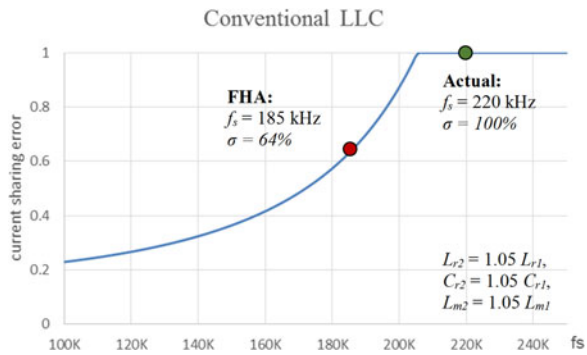

Fig. 16. Current sharing error versus switching frequency of conventional two-phase *LLC* converter.

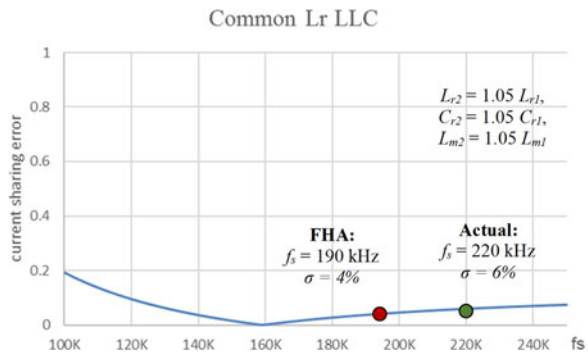

Fig. 17. Current sharing error versus switching frequency of two-phase common inductor *LLC* converter.

Fig. 16 shows the current sharing error changing with the switching frequency in conventional two-phase *LLC* converter. The parameter tolerance between phase 1 and phase 2 is that $L_{r2} = 1.05\,L_{r1}$, $C_{r2} = 1.05\,C_{r1}$, and $L_{m2} = 1.05\,L_{m1}$ (worst case). Take 400 V operation as an example, in FHA method, the predicted switching frequency is 185 kHz, at which the current sharing error is 64%. The actual switching frequency measured in PSIM is 220 kHz, and the current sharing error is 100%. It could be observed that for conventional *LLC* converter, the current sharing error has a steep curve versus switching frequency. In other words, a small change of switching frequency will cause a large change of output current. Thus, the deviation between FHA and PSIM results is relatively large.

Fig. 17 shows the current sharing error changing with switching frequency in common inductor two-phase *LLC* converter. Still use 400 V operation as an example, the FHA predicted

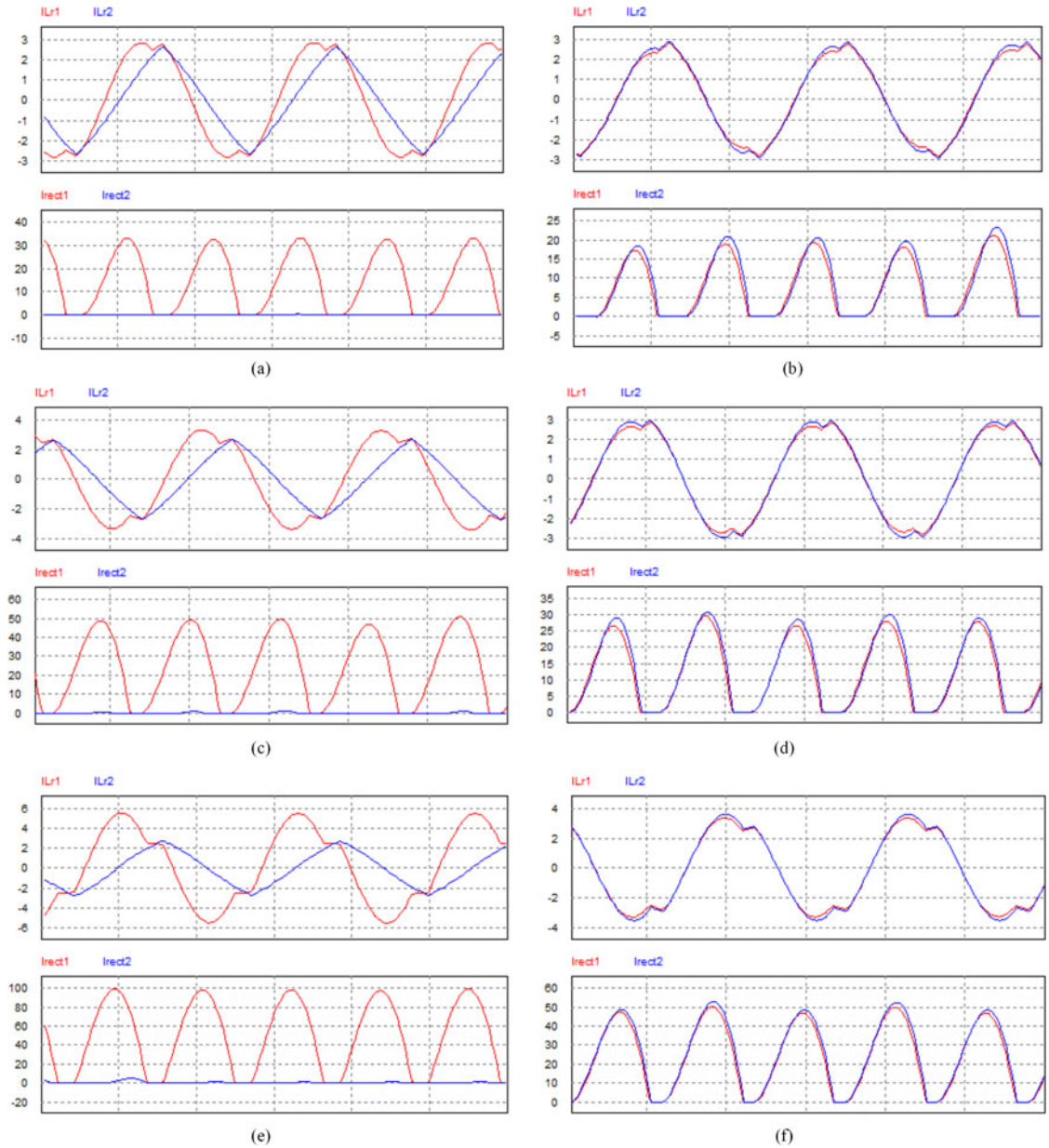

Fig. 18. Simulation for conventional and common inductor two-phase *LLC* converter at 400 V input and different load conditions. (a) Conventional *LLC* converter at 400 V input and total 15 A load. (b) Common inductor *LLC* converter at 400 V input and total 15 A load. (c) Conventional *LLC* converter at 400 V input and total 25 A load. (d) Common inductor *LLC* converter at 400 V input and total 25 A load. (e) Conventional *LLC* converter at 400 V input and total 50 A load. (f) Common inductor *LLC* converter at 400 V input and total 50 A load.

switching frequency is around 190 kHz and the current sharing error is 4%. The actual switching frequency in PSIM simulation is 220 kHz, at which the corresponding current sharing error reduces to 6% in Fig. 17. The value "6%" is not exactly the same with the actual current sharing error as 2% shown in Table IV. The reason is that Fig. 17 is still from FHA prediction. The key point here is that the curve is rather flat. Thus, the deviation between FHA and the PSIM results is small.

TABLE VII
EXPERIMENTAL PROTOTYPE PARAMETERS

	Resonant Inductor L_r	Resonant capacitor C_r	Magnetizing inductor L_m	Leakage Inductance L_e
Phase 1	22.5 μH	12.3 nF	95 μH	6 μH
Phase 2	24.5 μH (+8.9%)	12.7 nF (+3.3%)	92 μH (–3.2%)	6.5 μH (+8.3%)

D. Simulation Results for Experimental Prototype Parameters

The parameters and tolerances based on experimental prototype are shown in Table VII. It is the worst case as the tolerance direction on L_r and L_m is opposite. The leakage inductor of transformer is now taken into consideration. The design total power is 600 W (300 W*2).

Fig. 18 shows the simulation waveforms of the conventional and proposed two-phase *LLC* converter at 400 V input and total

TABLE VIII
CURRENT SHARING ERROR AT EXPERIMENTAL PARAMETER TOLERANCE

		Conventional two-phase *LLC*				Common inductor two-phase *LLC*			
Totalcurrent	Phase	I_{Lr_rms}	σ_{resonant}	I_{rect_ave}	σ_{load}	I_{Lr_rms}	σ_{resonant}	I_{rect_ave}	σ_{load}
15A	Phase 1	2.1 A	13.5%	14.8 A	97.3%	1.9 A	2.6%	7.15 A	4.7%
	Phase 2	1.6 A		0.2 A		2.0 A		7.85 A	
25A	Phase 1	2.41 A	18.7%	24.7 A	97.6%	2.18 A	2.7%	12 A	4%
	Phase 2	1.65 A		0.3 A		2.3 A		13 A	
50A	Phase 1	3.61 A	36%	49.5 A	98%	2.4 A	2.6%	24.3 A	2.8%
	Phase 2	1.69 A		0.5 A		2.53 A		25.7 A	

15, 25, and 50 A load current, repetitively. A common inductor two-phase *LLC* converter could achieve significantly improved load current sharing.

Table VIII shows the resonant current sharing error σ_{resonant} and load current sharing error σ_{load} based on the prototype parameters and tolerances of conventional two-phase *LLC* converter and common inductor two-phase *LLC* converter at 400 V and different load conditions.

The load current sharing error is almost 100% in conventional two-phase *LLC* resonant converter, which means only one phase provides total power. The load current sharing error is reduced to around 2.8% in common inductor two-phase *LLC* resonant converter at full load.

In Table VIII, it is observed that the resonant current sharing error is generally lower than the load current sharing error due to the existence of the current sharing error in the primary side. However, at heavy load, when the resonant current sharing error is low (such as smaller than 5%), the load current sharing error becomes very reasonable. Thus, it is believed that good resonant current sharing guarantees good load current sharing at heavy load.

V. EXPERIMENT RESULTS

A 600-W two-phase *LLC* converter prototype using common inductor current sharing technology is built to verify the feasibility and to demonstrate the advantages of the proposed method. The circuit diagram is shown in Fig. 8. The resonant tank parameter is designed based on the traditional design method for a single-phase *LLC* resonant converter. Thus, the design of the proposed multiphase *LLC* resonant converter is same as the single-phase *LLC* converter. The prototype parameters are shown in Table IX. In experimental prototype, the current on the secondary side is very high, and the PCB track should be as short as possible. Thus, it is not appropriate or easy to measure the load current of each phase directly. As mentioned above, good resonant current sharing means good load current sharing. Resonant currents are measured as current sharing performance evaluation.

Fig. 19 shows the experiment waveform of the conventional two-phase *LLC* converter at 15 and 25 A total load current. Channel 1 is the output voltage. Channels 3 and 4 are the resonant current of two phases. The resonant current i_{Lr2} is almost triangular waveform (as magnetizing current for the transformer),

TABLE IX
PROTOTYPE SPECIFICATIONS

Switching frequency	180–270 kHz
Input Voltage	340–400 V
Output Voltage	12 V
Output Power	300 W × 2
Transformer Ratio n	20:1
Output Capacitance	1790 μF
Series Capacitance (C_r)	12 nF 13 nF
Resonant Inductance (L_r)	22.5 μH(Phase1) 24.5 μH(Phase2)
Leakage Inductance (L_e)	6 μH(Phase1) 6.5 μH(Phase2)
Magnetizing Inductance (L_m)	95 μH(Phase1) 92 μH(Phase2)
Output Capacitance	1790 μF (100 μF× 8 + 330 μF× 3)
Half-bridge MOSFET	IPB60R190C6
SR MOSFET	BSC011N03LS

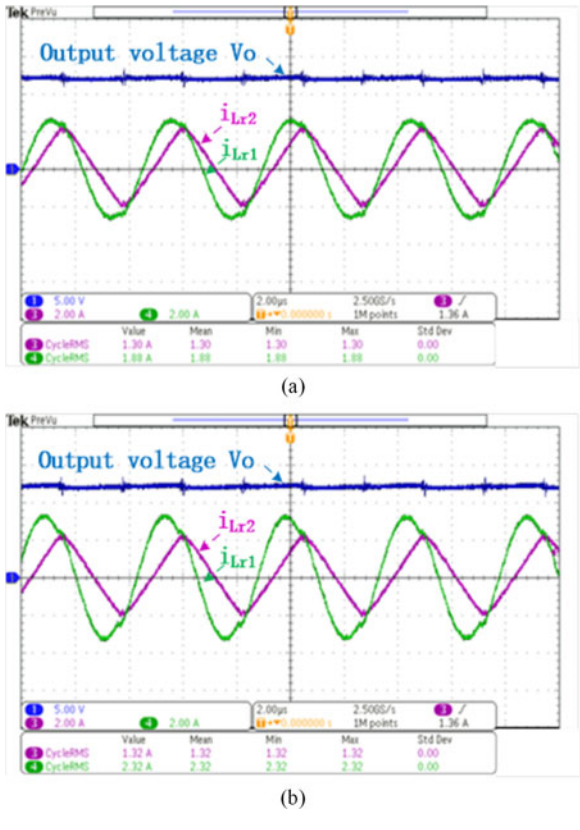

Fig. 19. Experimental waveform of conventional two-phase *LLC* converter. (a) Steady state at 15 A load. (b) Steady state at 25 A load Ch1: output voltage; Ch3: resonant current of phase 2; Ch4: resonant current of phase 1.

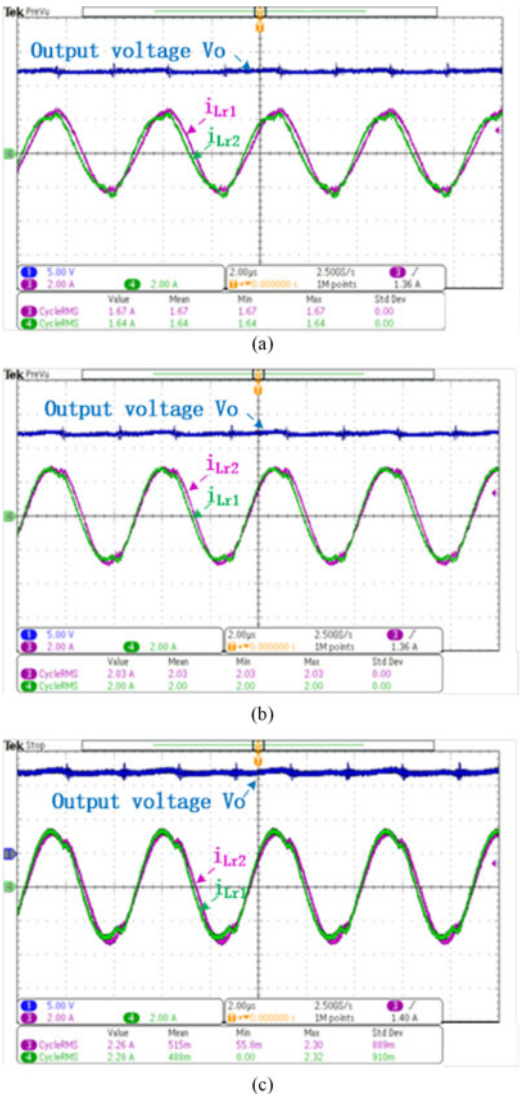

Fig. 20. Experimental waveform of proposed two-phase *LLC* converter. (a) Steady state at 15 A load. (b) Steady state at 25 A load. (c) Steady state at 50 A load Ch1: output voltage; Ch3: resonant current of phase 2; Ch4: resonant current of phase 1.

which means phase 2 does not provide the power for output load in Fig. 19(a) and (b).

Fig. 20 shows the experimental waveform of proposed common inductor two-phase *LLC* converter. The resonant current i_{Lr1} and i_{Lr2} is almost same at 15, 25, and 50 A load. A very small angle difference between them is shown at different load.

To show the current sharing performance, the resonant current and resonant current sharing error are shown in Figs. 21 and 22 for both conventional and proposed converter.

The resonant current sharing error increases from 10% to 28% for load power from 5 to 25 A for conventional two-phase *LLC* converter in Fig. 21. The resonant current sharing error is reduced from 2.3% to 0.44% for the proposed current sharing method when load power changes from 5 to 50 A in Fig. 22. The resonant current sharing error can be significantly reduced using the proposed method. Good current sharing performance

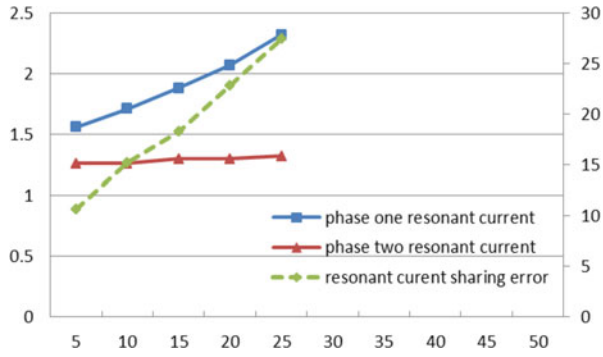

Fig. 21. Resonant current of conventional two-phase *LLC* converter.

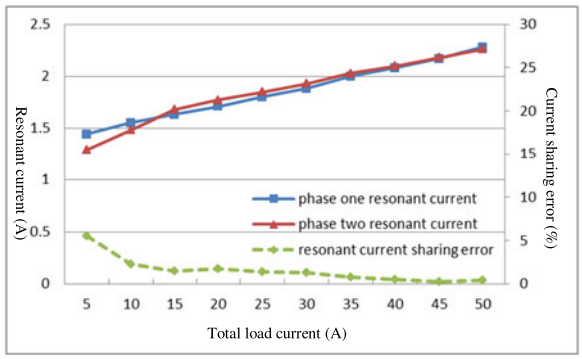

Fig. 22. Resonant current of proposed two-phase *LLC* converter.

can be achieved based on the common inductor two-phase *LLC* converter.

VI. Conclusion

A new, common inductor current sharing strategy for multiphase *LLC* resonant converter is proposed. The series resonant inductors in each *LLC* converter are connected in parallel. No additional components are needed to achieve current sharing. Mathematical model is built based on FHA to analyze the current sharing characteristics of both conventional and proposed two-phase *LLC* converter. The analysis results show that the current sharing error is significantly reduced using the proposed method. A two-phase *LLC* converter prototype with 300 W per phase is built using the common inductor current sharing method. The simulation and experiment results show that the circulating resonant current reduces 63 times and is only 0.44% at 600 W total load power with the proposed method.

References

[1] B. Yang, "Topology investigation for front end DC/DC power conversion for distributed power system," Ph.D. dissertation, Dept. Elect. Comput. Eng., Virginia Polytech. Inst. Stage Univ., Blacksburg, VA, USA, 2003.

[2] Y. Zhang, D. Xu, M. Chen, Y. Han, and Z. Du, "LLC resonant converter for 48 V to 0.9 V VRM," in *Proc. IEEE 35th Annu. Power Electron. Spec. Conf.*, 2004, vol. 3, pp. 1848–1854.

[3] B. Yang, F. C. Lee, A. J. Zhang, and H. Guisong, "LLC resonant converter for front end DC/DC conversion," in *Proc. IEEE 17th Annu. Appl. Power Electron. Conf. Expo.*, 2002, vol. 2, pp. 1108–1112.

[4] I. Batarseh, "Resonant converter topologies with three and four energy storage elements," *IEEE Trans. Power Electron.*, vol. 9, no. 1, pp. 64–73, Jan. 1994.

[5] R. Severns, "Topologies for three element resonant converters," in *Proc. 5th Annu. Appl. Power Electron. Conf. Expo.*, 1990, pp. 712–722.
[6] R. P. Severns, "Topologies for three-element resonant converters," *IEEE Trans. Power Electron.*, vol. 7, no. 1, pp. 89–98, Jan. 1992.
[7] T. B. Soeiro, J. Muhlethaler, J. Linner, P. Ranstad, and J. W. Kolar, "Automated design of a high-power high-frequency LCC resonant converter for electrostatic precipitators," *IEEE Trans. Ind. Electron.*, vol. 60, no. 11, pp. 4805–4819, Nov. 2013.
[8] L. Zhe, P. Chun-Yoon, K. Jung-Min, and K. Bong-Hwan, "High-power-factor single-stage LCC resonant inverter for liquid crystal display backlight," *IEEE Trans. Ind. Electron.*, vol. 58, no. 3, pp. 1008–1015, Mar. 2011.
[9] M. C. Tsai, "Analysis and implementation of a full-bridge constant-frequency LCC-type parallel resonant converter," *Proc. Inst. Elect. Eng., Electr. Power Appl.*, vol. 141, no. 3, pp. 121–128, May 1994.
[10] I. Batarseh, R. Liu, C. Q. Lee, and A. K. Upadhyay, "Theoretical and experimental studies of the LCC-type parallel resonant converter," *IEEE Trans. Power Electron.*, vol. 5, no. 2, pp. 140–150, Apr. 1990.
[11] X. Qu, S.-C. Wong, and C. K. Tse, "An improved LCLC current-source-output multistring LED driver with capacitive current balancing," *IEEE Trans. Power Electron.*, vol. 30, no. 10, pp. 5783–5791, Oct. 2015.
[12] N. Shafiei, M. Pahlevaninezhad, H. Farzanehfard, and S. R. Motahari, "Analysis and implementation of a fixed-frequency LCLC resonant converter with capacitive output filter," *IEEE Trans. Ind. Electron.*, vol. 58, no. 10, pp. 4773–4782, Oct. 2011.
[13] C. M. Bingham, A. Yong Ann, M. P. Foster, and D. A. Stone, "Analysis and control of dual-output LCLC resonant converters with significant leakage inductance," *IEEE Trans. Power Electron.*, vol. 23, no. 4, pp. 1724–1732, Jul. 2008.
[14] H. M. Suryawanshi and S. G. Tarnekar, "Modified LCLC-type series resonant converter with improved performance," *Proc. Inst. Elect. Eng., Electr. Power Appl.*, vol. 143, no. 5, pp. 354–360, Sep. 1996.
[15] Y. Chen, H. Wang, Z. Hu, Y.-F. Liu, J. Afsharian, and Z. A. Yang, "LCLC resonant converter for hold up mode operation," in *Proc. IEEE Energy Convers. Congr. Expo.*, 2015, pp. 556–562.
[16] M. T. Zhang, M. M. Jovanovic, and F. C. Y. Lee, "Analysis and evaluation of interleaving techniques in forward converters," *IEEE Trans. Power Electron.*, vol. 13, no. 4, pp. 690–698, Jul. 1998.
[17] M. T. Zhang, M. M. Jovanovic, and F. C. Lee, "Analysis, design, and evaluation of forward converter with distributed magnetics-interleaving and transformer paralleling," in *Proc. 10th Annu. Appl. Power Electron. Conf. Expo.*, 1995, vol. 1, pp. 315–321.
[18] R. Hermann, S. Bernet, S. Yongsug, and P. K. Steimer, "Parallel connection of integrated gate commutated thyristors (IGCTs) and diodes," *IEEE Trans. Power Electron.*, vol. 24, no. 9, pp. 2159–2170, Sep. 2009.
[19] J. Rabkowski, D. Peftitsis, and H. P. Nee, "Parallel-operation of discrete SiC BJTs in a 6-kW/250-kHz DC/DC boost converter," *IEEE Trans. Power Electron.*, vol. 29, no. 5, pp. 2482–2491, May 2014.
[20] Z. Hu, Y. Qiu, Y.-F. Liu, and P. C. Sen, "An interleaving and load sharing method for multiphase LLC converters," in *Proc. IEEE 28th Annu. Appl. Power Electron. Conf. Expo.*, 2013, pp. 1421–1428.
[21] H. Figge, T. Grote, N. Froehleke, J. Boecker, and P. Ide, "Paralleling of LLC resonant converters using frequency controlled current balancing," in *Proc. IEEE Power Electron. Spec. Conf.*, 2008, pp. 1080–1085.
[22] K. Bong-Chul, P. Ki-Bum, and M. Gun-Woo, "Analysis and design of two-phase interleaved LLC resonant converter considering load sharing," in *Proc. IEEE Energy Convers. Congr. Expo.*, 2009, pp. 1141–1144.
[23] Z. Hu, Y. Qiu, L. Wang, and Y.-F. Liu, "An interleaved LLC resonant converter operating at constant switching frequency," in *Proc. IEEE Energy Convers. Congr. Expo.*, 2012, pp. 3541–3548.
[24] Z. Hu, Y. Qiu, L. Wang, and Y.-F. Liu, "An interleaved LLC resonant converter operating at constant switching frequency," *IEEE Trans. Power Electron.*, vol. 29, no. 6, pp. 2931–2943, Jul. 2014.
[25] Z. Hu, Y. Qiu, Y.-F. Liu, and P. C. Sen, "A control strategy and design method for interleaved LLC converters operating at variable switching frequency," *IEEE Trans. Power Electron.*, vol. 29, no. 8, pp. 4426–4437, Aug. 2014.
[26] E. Orietti, P. Mattavelli, G. Spiazzi, C. Adragna, and G. Gattavari, "Two-phase interleaved LLC resonant converter with current-controlled inductor," in *Proc. Brazilian Power Electron. Conf.*, 2009, pp. 298–304.
[27] B.-C. Kim, K.-B. Park, C.-E. Kim, and G.-W. Moon, "Load sharing characteristic of two-phase interleaved LLC resonant converter with parallel and series input structure," in *Proc. Energy Convers. Congr. Expo.*, 2009, pp. 750–753.
[28] F. Jin, F. Liu, X. Ruan, and X. Meng, "Multi-phase multi-level LLC resonant converter with low voltage stress on the primary-side switches," in *Proc.2014 IEEE Energy Convers. Congr. Expo.*, 2014, pp. 4704–4710.
[29] H. Wang, Y. Chen, Y.-F. Liu, J. Afsharian, and A. Z. Yang, "A common inductor multi-phase LLC resonant converter," in *Proc. 2015 IEEE Energy Convers. Congr. Expo.*, 2015, pp. 548–555.
[30] E. Orietti, P. Mattavelli, G. Spiazzi, C. Adragna, and G. Gattavari, "Analysis of multi-phase LLC resonant converters," in *Proc. Brazilian Power Electron. Conf.*, 2009, pp. 464–471.
[31] E. Orietti, P. Mattavelli, G. Spiazzi, C. Adragna, and G. Gattavari, "Current sharing in three-phase LLC interleaved resonant converter," in *Proc. IEEE Energy Convers. Congr. Expo.*, 2009, pp. 1145–1152.
[32] B. C. Kim, K. B. Park, C. E. Kim, and G. W. Moon, "Load sharing characteristic of two-phase interleaved LLC resonant converter with parallel and series input structure," in *Proc. Energy Convers. Congr. Expo.*, 2009, pp. 750–753.
[33] Y. Gang, P. Dubus, and D. Sadarnac, "Analysis of the load sharing characteristics of the series-parallel connected interleaved LLC resonant converter," in *Proc. 13th Int. Conf. Optim. Electr. Electron. Equip.*, 2012, pp. 798–805.
[34] H. Wang, Y. Chen, and Y.-F. Liu, "A passive-impedance-matching concept for multi-phase resonant converter," in *Proc. Appl. Power Electron. Conf. Expo.*, 2016, pp. 899–906.
[35] H. Wang *et al.*, "An algorithm to analyze circulating current for multi-phase resonant converter," in *Proc. Appl. Power Electron. Conf. Expo.*, 2016, pp. 899–906.
[36] I. O. Lee and G. W. Moon, "The k-Q analysis for an LLC series resonant converter," *IEEE Trans. Power Electron.*, vol. 29, no. 1, pp. 13–16, Jan. 2014.

Hongliang Wang (M'12–SM'15) received the B.Sc. degree in electrical engineering from Anhui University of Science and Technology, Huainan, China, in 2004, and the Ph.D. degree in electrical engineering from Huazhong University of Science and Technology, Wuhan, China, in 2011.

From 2004 to 2005, he was an Electrical Engineer at Zhejiang Hengdian Thermal Power Plant. From 2011 to 2013, he was a Senior System Engineer at Sungrow Power Supply, Co., Ltd. He is currently a Postdoctoral Fellow at Queen's University, Kingston, ON, Canada, since 2013. He has published more than 50 papers in conferences and journals. He is the inventor/coinventor of 41 China issued patents, 15 U.S. patents, and 6 PCT patents pending. His research in the area of power electronics, including digital control, modulation, and multilevel topology of inverter for photovoltaic application and microgrids application, resonant converters and server power supplies, and LED drivers.

Dr. Wang is currently a Senior Member of China Electro-Technical Society and a Senior Member of China Power Supply Society (CPSS). He serves as a member of CPSS Technical Committee on Standardization; a member of CPSS Technical Committee on Renewable Energy Power Conversion; a Vice Chair of Kingston Section, IEEE; a Session Chair of ECCE 2015; a TPC member of ICEMS2012, and a China Expert Group Member of IEC standard TC8/PT 62786.

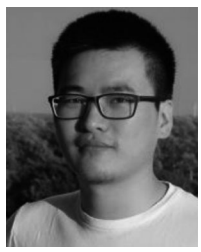

Yang Chen (S'14) received the B.Sc. degree in electrical engineering, in 2011, and the M.Sc. degree in electrical engineering, in 2013, both from Beijing Institute of Technology, Beijing, China. He is currently working toward the Ph.D. degree in electrical engineering at Queen's University, Kingston, ON, Canada.

His research interests include topology, control, and design of resonant converters in ac–dc and dc–dc fields, power factor correction technology, and digital control.

Yan-Fei Liu (M'94–SM'97–F'13) received the bachelor's and master's degree from the Department of Electrical Engineering from Zhejiang University, Hangzhou, China, in 1984 and 1987, and the Ph.D. degree from the Department of Electrical and Computer Engineering, Queen's University, Kingston, ON, Canada, in 1994.

He was a Technical Advisor with the Advanced Power System Division, Nortel Networks, Ottawa, ON, Canada, from 1994 to 1999. Since 1999, he has been with Queen's University, where he is currently a Professor with the Department of Electrical and Computer Engineering. He has authored more than 200 technical papers in the IEEE transactions and conferences and holds 20 U.S. patents. He is also a principal contributor for two IEEE standards. His current research interests include digital control technologies for high efficiency, fast dynamic response dc–dc switching converter and ac–dc converter with power factor correction, resonant converters and server power supplies, and LED drivers.

Dr. Liu received Premier's Research Excellence Award in 2000 in Ontario and the Award of Excellence in Technology in Nortel in 1997. He serves as an Editor of the IEEE JOURNAL OF EMERGING AND SELECTED TOPICS OF POWER ELECTRONICS (IEEE JESTPE) since 2013, an Associate Editor of the IEEE TRANSACTIONS ON POWER ELECTRONICS since 2001, and a Guest Editor-in-Chief of the special issue of Power Supply on Chip of the IEEE TRANSACTIONS ON POWER ELECTRONICS from 2011 to 2013. He also served as a Guest Editor for special issues of JESTPE: Miniaturization of Power Electronics Systems in 2014 and Green Power Supplies in 2016. He serves as the Co-General Chair of ECCE 2015 held in Montreal, QC, Canada, in September 2015. He will be the General chair of ECCE 2019 to be held in Baltimore, MD, USA. He has been the Chair of PELS Technical Committee on Control and Modeling Core Technologies since 2013 and the Chair of PELS Technical Committee on Power Conversion Systems and Components from 2009 to 2012.

Jahangir Afsharian received the B.S. and M.S. degrees in electrical engineering, in 2006 and 2009, respectively, from Ryerson University, Toronto, ON, Canada, where he is currently working toward the Ph.D. degree.

From 2009 to 2011, he was a Research and Development Engineer in the Communications and Power Industries, Georgetown, ON, Canada, where he was involved on the design of resonant converter *LCC* and high-voltage transformer for X-ray medical equipment. Since end of 2011, he has been a Senior Electrical Engineer in the Advanced Development Group, Murata Power solution, where he is involved in the power electronics ac–dc power factor correction and dc–dc converter. His current research interests include three-phase matrix-based rectifier for battery charger and data center applications.

Zhihua Yang was born in Hubei, China. He received the B.S. degree from Hubei Institute of Technology, Hubei, China, in 1993, and the M.S. degree from Queen's University, Kingston, ON, Canada, in 2005, both in electrical engineering.

He was a Design Engineer with Wuhan Zhouji Telecom Power Supply Corporation from 1993 to 2002. During 2005–2007, he was a Design Engineer with the Advanced Research Center, Paradigm Electronics, Inc., Canada. In 2007, he joined Murata Power Solutions, Inc., Markham, ON, where he was a Design Engineer, Senior Design Engineer, and Principal Design Engineer. He is currently the Director of Product Development at Murata power solutions, Inc. His research interest is in high switching frequency, high power density, and high-efficiency switching mode power suppliers.